# INFORMATION TO USERS

This manuscript has been reproduced from the microfilm master. UMI films the text directly from the original or copy submitted. Thus, some thesis and dissertation copies are in typewriter face, while others may be from any type of computer printer.

**The quality of this reproduction is dependent upon the quality of the copy submitted.** Broken or indistinct print, colored or poor quality illustrations and photographs, print bleedthrough, substandard margins, and improper alignment can adversely affect reproduction.

In the unlikely event that the author did not send UMI a complete manuscript and there are missing pages, these will be noted. Also, if unauthorized copyright material had to be removed, a note will indicate the deletion.

Oversize materials (e.g., maps, drawings, charts) are reproduced by sectioning the original, beginning at the upper left-hand corner and continuing from left to right in equal sections with small overlaps. Each original is also photographed in one exposure and is included in reduced form at the back of the book.

Photographs included in the original manuscript have been reproduced xerographically in this copy. Higher quality 6" x 9" black and white photographic prints are available for any photographs or illustrations appearing in this copy for an additional charge. Contact UMI directly to order.

UMI

University Microfilms International
A Bell & Howell Information Company
300 North Zeeb Road Ann Arbor MI 48106-1346 USA
313 761-4700 800 521-0600

Order Number 9218255

# Analysis of signaling by human FcgammaRIIA and of its potential role in autoimmune diseases

Odin, Joseph Alan, Ph.D.

City University of New York, 1992



U·M·I
300 N. Zeeb Rd.
Ann Arbor, MI 48106

# Analysis of Signaling by Human FcgammaRIIA and of Its Potential Role in Autoimmune Diseases

by

Joseph Alan Odin

A dissertation submitted to the Graduate Faculty in Biomedical Sciences in partial fulfillment of the requirements for the degree of Doctor of Philosophy, The City University of New York.

1992

This manuscript has been read and accepted by the Graduate Faculty in Biomedical Sciences in satisfaction of the dissertation requirement for the degree of Doctor of Philosophy.

1/24/92
Date

Chair of Examining Committee

1/27/92
Date

Executive Officer

Supervisory Committee

The City University of New York

## Abstract

# Analysis of Signaling by Human FcgammaRIIA and of Its Potential Role in Autoimmune Diseases

by

Joseph Alan Odin

Adviser: Jay Unkeless, Ph.D.

The activation mechanism of macrophages following the binding of IgG complexes to Fc receptors ($Fc_\gamma R$) is a complex and poorly understood process. Cross-linking of $Fc_\gamma Rs$ results in multiple cellular responses that are important for cell-mediated immunity, including phagocytosis and the release of oxidative metabolites. The analysis of a series of truncations of human $Fc_\gamma RIIA$, which were expressed in a mouse macrophage-like cell line, presented here indicates that separate cytoplasmic regions are required for internalization of antibody-FcR complexes versus internalization of opsonized erythrocytes and an increase in $[Ca^{2+}]_i$. The cytoplasmic region required for antibody-FcR internalization extended from $Arg^{234}$ to $Asp^{264}$, whereas internalization of opsonized erythrocytes and the increase in $[Ca^{2+}]_i$ were dependent on the final 17 COOH-terminal amino acids, $Lys^{265}$ to $Asn^{281}$. The internalization of opsonized erythrocytes was dependent on the increase in calcium levels. The internalization of antibody-FcR complexes was dependent on protein kinase

C and tyrosine kinase activity, and all functional responses required factors found in macrophages but not in fibroblasts. These results suggest a signal transduction model in which huFc$_\gamma$RIIA cross-linked by immune complexes couple directly to multiple effector systems, each of which initiates a distinct biological response.

Recently, high levels of anti-Fc$_\gamma$R antibodies were identified in the sera of patients with autoimmune diseases and in several mouse autoimmune strains by using a recombinant, soluble murine Fc$_\gamma$RII to screen the sera (1). To enhance the screening of sera from human patients, large quantities (> 1 mg/L) of a recombinant, soluble huFc$_\gamma$RIIA were expressed and purified from transfected CHO cells. An initial screening of autoimmune sera showed some positive reactivity with this soluble huFc$_\gamma$RIIA.

## Acknowledgements

In this work, I have greatly benefitted from the insightful guidance of my adviser, Dr. Jay Unkeless, whose unfailing optimism and support made these past several years a very rewarding experience. All past and current members of Dr. Unkeless' laboratory were a pleasure to work with as well. In particular, Dr. Peter Boros and Catherine Painter provided invaluable advice and assistance concerning many aspects of this project. Additionally, I am grateful for the aid and suggestions of Drs. Jeffrey Edberg and Robert Kimberly in analyzing intracellular calcium fluxes and erythrocyte phagocytosis. I thank A. Pizzimenti, Dr. J. Cheng, and D. Yang for their technical assistance beyond the call of duty and their good humor. I am also indebted as usual to my parents, who have always encouraged me to do my best. Finally, I wish to thank my wife, Christine, for both her advice on and her much needed distraction from my thesis work.

## Table of Contents

# List of Tables

# List of Figures

# I. Overview of Receptors for IgG

## Introduction

In this thesis, structure-function analysis of a human $Fc_{\gamma}R$ and the development of a soluble human $Fc_{\gamma}R$ are reported. To facilitate greater understanding of the problems addressed, a summary of pertinent facts concerning $Fc_{\gamma}Rs$ followed by an in depth analysis of the structure, function, signaling, and autoimmune disease role of these receptors is presented.

In the late 19th century, Eli Metchnikoff first recognized the importance of mononuclear phagocytes in combatting inflammatory disease. These cells were named macrophages due to their ability to engulf large particles. Later, it was discovered that macrophages, when activated, utilize multiple means to eliminate "foreign" or defective particles. While neutrophils primarily target bacteria, macrophages dispose of a wide range of cells and debris. Macrophages, which are found in nearly all tissues, also play a major role in tumor surveillance and are key antigen presenting cells. Activation of macrophages requires stimulation of surface receptors such as complement receptors and receptors for the Fc domain of IgG, $Fc_{\gamma}Rs$. Through these receptors, macrophages forge a link between humoral immunity and cell-mediated immunity. Defective $Fc_{\gamma}R$-mediated macrophage function occurs in some autoimmune diseases, though it is not clear if this is a cause or a result of the disease state.

Fc receptors for IgG, $Fc_{\gamma}Rs$, are a family of receptors that specifically bind IgG via the Fc domain and mediate cellular functions (Table 1). These functions can be grouped into three areas: cellular immune defense and lymphocyte regulation,

**Table 1.** Properties of human (hu) and mouse (mu) $Fc_\gamma Rs$ (2).

| Receptor | Mol. Wt. (kDa) | Cell Distrib. | Affinity | mAbs |
|---|---|---|---|---|
| $huFc_\gamma RI$ | 72 | monocyte, macrophage, U937, HL-60, IFNγ treated neutrophils | high | 32.2, 62, 22, 44, 10.1, FR51 |
| $huFc_\gamma RIIA$ | ~40 | U937, monocyte, neutrophil, platelet | low | IV.3, 2E1, KB56, 41H.16 |
| $huFc_\gamma RIIB_1$-$B_3$ | ~40 | B cell, U937, monocyte, neutrophil, placenta | low | KB61, 41H.16, 2E1, IV.3 |
| $huFc_\gamma RIIC$ | ~40 | B cell, U937, monocyte, neutrophil | low | same as above |
| $huFc_\gamma RIIIA$ | 50-70 | monocyte?, macrophage, NK | low | 3G8, CLB-FcR-GRAN1, B73.1 Leu-11a, Leu-11b, Leu-11c |
| $huFc_\gamma RIIIB$ | 50-70 | neutrophil | low | same as above |
| $muFc_\gamma RI$ | ~70 | macrophage | high | (none) |
| $muFc_\gamma RII_1$ | 50-70 | lymphoid cells | low | 2.4G2 |
| $muFc_\gamma RII_2$ | 50-70 | lymphoid and myeloid cells | low | 2.4G2 |
| $muFc_\gamma RIII$ | 50-70 | macrophage, NK, mesangial cells | low | 2.4G2 |

immunoglobulin transcytosis, and autoimmune pathology. In cellular immune defense upon cross-linking by IgG aggregates, $Fc_\gamma Rs$ activate a variety of leukocyte responses such as phagocytosis, antibody-dependent cell cytotoxicity (ADCC), and the release of lysosomal hydrolases, reactive oxygen metabolites, arachidonate metabolites, and other mediators of inflammation. Cross-linking of cell surface antibodies to membrane bound $Fc_\gamma Rs$ inhibits B cell differentiation (3,4). Though not yet tested, it seems likely that $Fc_\gamma Rs$ on neonatal rat gut epithelium (5) and syncytiotrophoblasts (6) are involved in transcytosis of immunoglobulin. Dysfunction of macrophage $Fc_\gamma Rs$ (7,8) as well as the presence of high titers of anti-$Fc_\gamma R$ immunoglobulin (1,9) have been reported in both human and mouse autoimmune diseases.

All FcRs, except CD23 ($Fc_\epsilon RII$), are members of the Ig supergene family and are homologous to each other. $Fc_\gamma Rs$ are class I membrane glycoproteins that span the cell membrane once, except $huFc_\gamma RIIIB$, which is anchored in the neutrophil plasma membrane by a glycan phosphatidyl inositol (GPI) moiety (10-14). Low avidity forms of membrane bound $Fc_\gamma Rs$ possess two extracellular Ig-like regions, whereas high avidity forms contain three Ig-like regions. Assigning functions to individual $Fc_\gamma Rs$ has been a challenging task since many share immunologically indistinguishable extracellular domains and their cellular distributions overlap considerably.

## $Fc_\gamma$Receptor Structure

### *$HuFc_\gamma RI$*

Human monocytes have 20,200 binding sites for human IgG1 and IgG3 with a $K_a$ of $\sim 8.6 \times 10^8\ M^{-1}$ (15,16). High affinity binding ($10^8$-$10^9\ M^{-1}$) of murine IgG

subclasses IgG2a and IgG3 to human monocytes has been shown as well (17). This high affinity receptor is univalent (as are all $Fc_\gamma Rs$) for human IgG1 (18). The receptor, now termed $huFc_\gamma RI$ (CD64), was purified by Sepharose-IgG affinity chromatography from monocytes (19,20). $HuFc_\gamma RI$ has a $M_r$ of 72 kDa as determined by SDS-PAGE. Treatment of the receptor with endo-$\beta$-N-acetylglucosaminidase F or N-glycanase yielded a core protein of 40 or 50 kDa, respectively (21,22). IFN-$\gamma$ treatment of neutrophils induces $huFc_\gamma RI$ expression (23,24).

Recent cloning of cDNAs for $huFc_\gamma RI$ showed that the extracellular domain contains six potential N-linked glycosylation sites and six cysteine residues, presumably disulfide linked to form three C2-set Ig-like regions (25). In contrast, $huFc_\gamma RII$ and $huFc_\gamma RIII$ encode only two Ig-like regions. The transmembrane domain is 21 residues long and the cytoplasmic domain is short and highly charged (25). Homology exists between the first two N-terminal Ig-like regions of $huFc_\gamma RI$ and the analogous domains of the low avidity $Fc_\gamma Rs$ (25,26). The uniqueness of the third domain and its conservation between human and mouse, as well as preliminary mutational analysis (25), suggest that this third membrane-proximal domain of $Fc_\gamma RI$ endows high affinity ligand binding capacity.

*$HuFc_\gamma RII$*

A second receptor on monocytes, $huFc_\gamma RII$, binds aggregated IgG with low avidity ($Ka = 1\text{-}3 \times 10^6\ M^{-1}$) and unlike $huFc_\gamma RI$ does not bind monomeric IgG (27). $HuFc_\gamma RII$ (CD32) was also initially purified by affinity chromatography of monocyte lysates on IgG-Sepharose (19). A protein of about 40 kDa was isolated that has since

been found on monocytes, neutrophils, platelets, B cells, eosinophils (28,29), basophils (30) and trophoblasts (6). The affinity with which huFc$_\gamma$RII on platelets binds IgG subclasses is the following: $IgG_1 = IgG_3 >> IgG_2 = IgG_4$ (31). In addition, only murine IgG1-sensitized erythrocytes were bound by huFc$_\gamma$RII-expressing cell lines, whereas previous work suggested that both murine IgG1 and IgG2b bound to huFc$_\gamma$RII (29).

Initial cDNA clones of huFc$_\gamma$RII were nearly identical with no differential splicing (32,33). The predicted class I membrane protein contains two C-2 set Ig-like extracellular domains with two potential N-linked glycosylation sites apiece. The observation that the anti-huFc$_\gamma$RII mAb IV.3 did not react with Daudi cells, although a 40 kDa huFc$_\gamma$R could be immunoprecipitated with a polyclonal anti-huFc$_\gamma$RII serum (34), suggested the possibility of isotypic variation. Subsequently, additional cDNA clones were isolated showing that at least three genes encode huFc$_\gamma$RII proteins (6,35-37). All of the huFc$_\gamma$RIIs (huFc$_\gamma$RIIA, huFc$_\gamma$RIIB, huFc$_\gamma$RIIC) have homologous extracytoplasmic domains and are most homologous to muFc$_\gamma$RII, especially huFc$_\gamma$RIIB.

HuFc$_\gamma$RIIA transcripts were found in neutrophils, cultured adherent monocytes, and various monocyte-like cell lines (36). Of five lymphoid cell lines (Daudi, Raji, AW RAMOS, IM-9, and MOLT-4), only the Burkitt lymphoma cell line Daudi expressed huFc$_\gamma$RIIA mRNA. This was unexpected since mAb IV.3 preferentially recognizes huFc$_\gamma$RIIA but does not bind to Daudi cells. HuFc$_\gamma$RIIB is expressed by B cells, and to a lesser extent neutrophils and cultured adherent monocytes (36). Both

huFc$_\gamma$RIIB and muFc$_\gamma$RII undergo differential splicing in their cytoplasmic domains (36). HuFc$_\gamma$RIIC is nearly identical to huFc$_\gamma$RIIB in its signal sequence and extracytoplasmic domains, but in its cytoplasmic domain and 3' untranslated region, huFc$_\gamma$RIIC has high homology to huFc$_\gamma$RIIA. The distribution of huFc$_\gamma$RIIC includes B cells, cultured adherent monocytes, and neutrophils (36).

*HuFc$_\gamma$RIII*

HuFc$_\gamma$RIII (CD16), binds IgG1 and IgG3 with a $K_a$ of $\sim 4 \times 10^6$ $M^{-1}$ (15) and is expressed on macrophages, NK cells, neutrophils, eosinophils, and some T cells (38). The $M_r$ of huFc$_\gamma$RIII on macrophages and NK cells varies between 50 and 70 kDa (39). Immunoprecipitation studies of NK and neutrophil cell lysates using a huFc$_\gamma$RIII-specific mAb followed by deglycosylation and SDS-PAGE revealed core proteins of different $M_r$ in the two cell types (24 kDa versus 20 kDa, respectively) (40). Subsequent cDNA cloning demonstrated that the NK cell transcribes an mRNA distinct from that of neutrophils (12-14,41,42). Thus, at least two genes encode huFc$_\gamma$RIIIs: huFc$_\gamma$RIIIB on neutrophils and huFc$_\gamma$RIIIA on NK cells and macrophages. Like huFc$_\gamma$RII, these low avidity Fc$_\gamma$RIIIs have only 2 C-2 set Ig-like extracellular domains.

HuFc$_\gamma$RIIIB, unlike all other Fc$_\gamma$Rs, is anchored to the neutrophil cell membrane via a GPI linkage and can be released from the cell membrane by treatment with a phosphoinositol-specific phospholipase C (12-14,41,42). Alteration of single amino acid in the GPI linkage domain of huFc$_\gamma$RIIIB results in anchorage of the protein by a transmembrane domain with a short cytoplasmic tail (43,44). Two

allotypes (NA1 and NA2) exist for huFc$_\gamma$RIIIB. Fetal-maternal mismatch for these allotypes can lead to autoimmune neutropenia in infants (45). HuFc$_\gamma$RIIIA has an extracellular domain that is >95% homologous to that of huFc$_\gamma$RIIIB but is a class I membrane glycoprotein with a single transmembrane domain and cytoplasmic domain (46).

*MuFc$_\gamma$RI*

Murine macrophages also posses both high and low affinity Fc$_\gamma$Rs. The number of high affinity ($K_a = 1.1 \times 10^8$) IgG2a binding sites is 84,000 on P388D$_1$ cells, 110,000 on normal mouse peritoneal macrophages, and 440,000 on thioglycollate-stimulated macrophages. This muFc$_\gamma$RI is trypsin sensitive, has a $M_r$ of about 42 kDa (47,48), and like huFc$_\gamma$RI, has 3 C-2 set Ig-like extracellular domains (25). The 23 amino acid transmembrane domain is followed by a carboxyl-terminal, 84 amino acid cytoplasmic tail. Southern analysis suggests that the receptor is encoded by only one gene (26).

*MuFc$_\gamma$RII and MuFc$_\gamma$RIII*

Mice express fewer low avidity Fc$_\gamma$R forms than humans, and none are GPI-anchored to the cell membrane. Studies of the low avidity muFc$_\gamma$Rs have been at the forefront of Fc$_\gamma$R research. The first anti-Fc$_\gamma$R mAb, 2.4G2, was directed against these receptors, which consequently were the first Fc$_\gamma$Rs to be cloned and expressed. After affinity chromatography of macrophage cell lysates on mAb 2.4G2-Sepharose (49), two major bands of ~60,000 and ~47,000 $M_r$ were visualized on SDS-PAGE. The isolated muFc$_\gamma$Rs demonstrated a broad ligand isotype specificity--binding complexes of either IgG1, IgG2b, or IgG2a (49). Amino acid sequencing of purified

receptor led to the isolation of three cDNA clones (50), now termed muFc$_\gamma$RIII (muFc$_\gamma$RII$\alpha$), muFc$_\gamma$RII$_1$ (muFc$_\gamma$R$\beta_1$), and muFc$_\gamma$RII$_2$ (muFc$_\gamma$RII$\beta_2$). MuFc$_\gamma$RII$_1$ and muFc$_\gamma$RII$_2$ are produced by differential splicing of a single gene (50). The encoded proteins are all class I integral membrane glycoproteins and are members of the immunoglobulin gene superfamily. The adjacent pairs of cysteines in the extracellular domains are disulfide linked (51,52) and each Ig-like domain has two sites for N-linked glycosylation (52). The proteins are 95% homologous in their extracellular domains, but differ in their cytoplasmic domains (50).

The muFc$_\gamma$RII transcripts are identical except for a 47 amino acid insertion in the cytoplasmic domain of muFc$_\gamma$RII$_1$ (50). MuFc$_\gamma$RII$_1$ is expressed in both myeloid and lymphoid cells, whereas expression of muFc$_\gamma$RII$_2$ is limited to macrophages (50,53,54). The expression of muFc$_\gamma$RII may be developmentally regulated since the muFc$_\gamma$RII$_1$ transcript was detected in immature macrophage cell lines, but only in two of three more mature macrophage lines (50). MuFc$_\gamma$RIII is expressed in macrophages, NK cells, and mesangial cells (53,55-57).

*Fc$_\gamma$R Subunits*

There is a highly conserved sequence in the transmembrane domains of muFc$_\gamma$RIII, huFc$_\gamma$RIIIA, and the $\alpha$ subunit of the high affinity rat Fc$_\epsilon$RI. The transmembrane domains of these receptors each share an identical stretch of eight amino acids, including a charged aspartyl residue in the middle of the lipid bilayer (13,50,58). Numerous investigators have had difficulty in expressing huFc$_\gamma$RIIIA and muFc$_\gamma$RIII cDNAs in transfected cell lines, while muFc$_\gamma$RII, which differs from

muFc$_\gamma$RIII only in the transmembrane and cytoplasmic domains, was readily expressed. Various mouse macrophage cell lines, which do not express Fc$_\epsilon$RI, express mRNA identical to the $\gamma$ subunit of raFc$_\epsilon$RI (59). Immunoprecipitation studies utilizing anti-muFc$_\gamma$RIII antibodies or mAbs revealed that radiolabeled muFc$_\gamma$RIII and a $\gamma$ subunit could be co-precipitated from detergent lysates of the J774 macrophage cell line (59). In addition, high level expression of muFc$_\gamma$RIII was obtained in cells cotransfected with $\gamma$ subunit cDNA and Fc$_\gamma$R cDNA (60).

Another line of investigation has led to the discovery of other Fc$_\gamma$R associated proteins. NK cells can carry out ADCC triggered by huFc$_\gamma$RIII-2, whereas in cytotoxic T lymphocytes, extracellular killing is triggered by the T cell receptor. The T cell antigen receptor is a multi-subunit protein composed of $\alpha$ and $\beta$ (or $\gamma$ and $\delta$) subunits and the CD3 complex ($\gamma$, $\delta$, $\epsilon$, and $\zeta_2$). Immunoprecipitation of NK cell membrane lysates using anti-$\zeta$ antibodies or anti-huFc$_\gamma$RIII antibodies coprecipitated $\zeta$ and Fc$_\gamma$RIII (61). Fixing of NK cells prior to immunoprecipitation extracted additional, unidentified proteins (62). Expression of huFc$_\gamma$RIIIA and muFc$_\gamma$RIII in transfected cells was enhanced by cotransfection with $\zeta$ cDNA (63). While $\gamma$ or $\zeta$ subunit coexpression has been shown to be required for efficient expression of huFc$_\gamma$RIII or muFc$_\gamma$RIII, no role for these subunits in signaling has yet been demonstrated. However, it is known that $\zeta$ is necessary for T cell receptor signaling (64).

**Fc$_\gamma$Receptor Functions**

Through the use of artificial immune complexes, the cellular responses following cross-linking of Fc$_\gamma$Rs, such as phagocytosis and ADCC, have been

extensively studied. However, only recently did the extensive heterogeneity among these receptors come to light. Therefore, much of the recent work on $Fc_\gamma Rs$ has centered on identifying which $Fc_\gamma R$ can mediate a particular response.

*Respiratory Burst*

Cross-linking of $huFc_\gamma RI$ on monocytes using mAb 32 with a secondary anti-IgG reagent results in $O_2^{-\cdot}$ production (65). Continuous $O_2^{-\cdot}$ production via $huFc_\gamma RI$ is dependent on continuous *de novo* formation of cross-linked $huFc_\gamma RI$ (66). Cross-linking of $huFc_\gamma RII$ can also trigger an oxidative burst from monocytes (65). $HuFc_\gamma RII$, not $huFc_\gamma RIIIA$, plays the major role in mediating $O_2^{-\cdot}$ release by neutrophils. Neutrophils from patients with paroxysmal nocturnal hematuria are $huFc_\gamma RIII$-negative but still mediate normal $O_2^{-\cdot}$ release in response to immune complexes (11). Digestion of neutrophils with elastase, which preferentially cleaves $huFc_\gamma RIII$, did not inhibit $O_2^{-\cdot}$ release triggered by immune complexes, whereas anti-$huFc_\gamma RII$ mAb IV.3 strongly inhibited release (67). Additionally, cross-linking of $huFc_\gamma RIIIB$ alone on neutrophils, when $huFc_\gamma RII$ was blocked by a specific mAb, did not induce a respiratory burst (68).

*Antibody-dependent Cell-mediated Cytotoxicity (ADCC)*

Recent work has shown that, with the exception of $huFc_\gamma RIIIB$, all three $Fc_\gamma Rs$ are capable of ADCC towards target cells. The $huFc_\gamma RI$-mediated ADCC response is dependent on effector cell type and maturity, as well as the target cell type (69-70). Inflammatory mediators may also be important, since exogenous C1q reconstitutes $Fc_\gamma R$-mediated ADCC and phagocytosis in mouse peritoneal macrophages (70).

HuFc$_\gamma$RI on monocytes and macrophages effects ADCC of both hybridoma and erythrocyte targets. IFN-$\gamma$ treatment augments huFc$_\gamma$RI-mediated ADCC by monocytes and induces that by neutrophils (69,70,73,74).

HuFc$_\gamma$RII plays a role in ADCC by neutrophils and monocytes as shown by the killing of mAb IV.3-bearing hybridomas (75) and murine IgG1 coated erythrocytes (76), respectively. Upon short term IFN-$\gamma$ or GM-CSF treatment (6 h) of neutrophils or GM-CSF treatment (6 h) of eosinophils, the huFc$_\gamma$RII-mediated cytotoxic potential of these cells is augmented, although neither lymphokine increases receptor number (77). Prolonged IFN-$\gamma$ treatment (18 h) of neutrophils activated killing of opsonized chicken erythrocytes (CE) mediated through all three huFc$_\gamma$R subclasses (77). However, neutrophils could not kill an anti-huFc$_\gamma$RIII hybridoma cell line.

HuFc$_\gamma$RIIIA on NK cells also mediates ADCC after cross-linking (78). Immune complex cross-linking of the receptor also induced transcription of the interleukin-2 receptor, IFN-$\gamma$, and TNF-$\alpha$, all of which further activate NK cells (79). Thus, in addition to acting as a trigger for ADCC on NK cells, the activation of huFc$_\gamma$RIIIA on NK cells also potentiates the Ig-independent, natural killer activity of NK cells. The ability of anti-LFA-1 (CD11a) antibodies to inhibit huFc$_\gamma$RIIIA mediated ADCC by NK cells suggests involvement of this adhesion receptor in effector cell-target cell apposition during NK-mediated ADCC (78). Similarly, in monocytes, blocking of LFA-1 inhibited ADCC mediated through cross-linking of huFc$_\gamma$Rs (71). HuFc$_\gamma$RIIIA on cultured monocytes is biochemically indistinguishable from that of NK cells (80), yet reports conflict over whether huFc$_\gamma$RIII is a trigger molecule for ADCC by

macrophages (71,80). The discrepancy in killing ability may be due to the different target cells and mAbs used in each study.

Early studies demonstrated the role of mouse macrophage $Fc_\gamma Rs$ in ADCC (81) and later, the primary mechanism of this cytotoxicity was shown to be oxidative and involved the release of $H_2O_2$ (82). ADCC of BCG-elicited macrophages was inhibited 70% by mAb 2.4G2, demonstrating the involvement of low avidity $muFc_\gamma Rs$ (83). NK cells express only $muFc_\gamma RIII$ and mediate ADCC (56). Also, $muFc_\gamma RIII$ is expressed in a TCR-$\gamma/\delta^+$ subset of murine dendritic epidermal cells which mediate ADCC (84).

*Phagocytosis*

Phagocytosis is the rapid, temperature-dependent delivery of immune complexes to lysosomes as seen in "professional" phagocytes such as neutrophils and macrophages. $HuFc_\gamma RI$ on monocytes, macrophages, and IFN-$\gamma$ treated neutrophils mediates phagocytosis of erythrocytes coated with heteroantibodies composed of Fab fragments of anti-$huFc_\gamma RI$ mAb and Fab fragments of anti-erythrocyte antibody (85). $HuFc_\gamma RII$ and not $huFc_\gamma RIIIB$ was required for phagocytosis of opsonized [$^{14}$C]-labeled *S. areus Wood* by neutrophils, since a mixture of anti-$huFc_\gamma RIII$ antibody and anti-$huFc_\gamma RII$ antibody did not inhibit phagocytosis any more than anti-$huFc_\gamma RII$ antibody alone (68).

The absolute or relative abundance of $muFc_\gamma RIII$ mRNA is increased by IFN-$\gamma$ in macrophage cell lines and macrophages, and this expression correlates with an increased phagocytic capacity (53). BCG-elicited macrophages do not express detectable levels of $muFc_\gamma RIII$ mRNA and are poorly phagocytic, whereas

phagocytically active resident and thioglycollate-elicited macrophages do express muFc$_\gamma$RIII (86).

Cyclic AMP may play a role in upregulation of muFc$_\gamma$RI expression, as well as in signaling for phagocytosis mediated by this receptor (87). A recent report showed that a casein-phosphorylation activity copurifies with IgG2a binding protein, and phagocytosis is inhibitable with heparin, a specific inhibitor of casein kinase II (88).

*Immune Complex Clearance in vivo*

The abilities of monomeric or aggregated IgG and mAb 2.4G2 to inhibit *in vivo* clearance of immune complexes in mice were studied (89). MAb 2.4G2, directed against low avidity muFc$_\gamma$Rs, was a very potent inhibitor of clearance of immune complexes and of IgG sensitized erythrocytes but also somewhat inhibited nonspecific clearance of heat damaged erythrocytes. While mAb 2.4G2 administration resulted in a depletion of complement as well (89), inhibition of clearance did not depend on complement mediated lysis of macrophages as the inhibition was still seen in a C5-deficient strain of mice (90).

A number of studies have demonstrated that huFc$_\gamma$RIIIA on macrophages in the spleen and on Kupffer cells is the primary receptor responsible for clearance of large immune complexes in humans. In chimpanzees, the anti-huFc$_\gamma$RIII mAb 3G8 inhibited clearance *in vivo* of autologous erythrocytes coated with antibody directed against a minor blood group antigen (8). MAb 3G8 has been tested as a potential therapeutic treatment for individuals with immune thrombocytic purpura, a disease in which patients secrete high levels of anti-platelet antibody (91). Treatment of one patient

resulted in a dramatic rise in platelet levels, returning to normal levels within two weeks. Unfortunately, a second treatment gave a much less dramatic response. Sensitization to the murine mAb may reduce its effectiveness.

*B Cell Regulation*

Stimulation of B cell differentiation by anti-$\mu$ $F(ab')_2$ is well described. However, when rabbit anti-$\mu$ IgG forms a ternary complex with sIg and $Fc_\gamma RII$ on the membrane of B cells, no differentiation takes place (4). The negative signal delivered by ligation of $Fc_\gamma R$ is relieved if anti-$\mu$ IgG and mAb 2.4G2 are added together, indicating the requirement for cross-linking of sIg to $Fc_\gamma R$ (4). Interestingly, the suppression of differentiation due to cross-linking of sIg and $Fc_\gamma R$ is abrogated by IL-4 (92). IL-4 acts to inhibit the binding of immune complexes to B cells. The mechanism responsible for the inhibition is not a reduction in receptors, because the number of $muFc_\gamma RII$ epitopes, determined by binding of mAb 2.4G2, remains unchanged (93). The inhibition might reflect altered mobility of $Fc_\gamma R$ on the plasma membrane.

*Functional Analysis of Transfected $Fc_\gamma Rs$*

The murine low avidity $Fc_\gamma Rs$ have been transfected into several $Fc_\gamma R$-nonexpressing cell lines, such as Madin-Darby canine kidney (MDCK) cells, and fibroblast cell lines, COS and CHO cells. The two splice forms of $muFc_\gamma RII$ were shown to have different and polarized patterns of surface expression in transfected MDCK cells, and $muFc_\gamma RII_2$ was preferentially capable of monovalent ligand transcytosis (94). $MuFc_\gamma RII_2$, transfected into COS and CHO cells, localized in clathrin coated pits, whereas $muFc_\gamma RII_1$ did not (95). This difference may be

responsible for the greater ability of transfected muFc$_\gamma$RII$_2$ to mediate endocytosis and lysosomal delivery of ligand (95). Presumably, the 47 amino acid cytoplasmic insertion of muFc$_\gamma$RII$_1$ interrupts a domain crucial for coated pit localization and transcytosis (94,95). However, internalization of *Toxoplasma gondii* by muFc$_\gamma$RII$_2$ transfected CHO cells was no better than that by muFc$_\gamma$RII$_1$ (96). Unfortunately, in most cases, transfection of Fc$_\gamma$Rs into Fc$_\gamma$R-nonexpressing cell lines has not resulted in functional receptors (personal communications).

**Fc Receptor Signaling**

The initial event in Fc$_\gamma$R signal transduction is receptor cross-linking. Monomeric IgG binding to Fc$_\gamma$Rs does not trigger immune responses. The paradigm for Fc$_\gamma$R cross-linking and action is the analysis of Fc$_\epsilon$RI (97), which demonstrated mast cell degranulation only after cross-linking. The more extensive the cross-linking, the greater the extent of granule release. Since cross-linking of Fc$_\gamma$Rs by antibodies directed at various extracellular epitopes can mediate cellular activation (2), most likely no conformational signal is transduced across the cell membrane following ligand binding. Yet, the diversity of the intracellular domains within an Fc$_\gamma$R subclass as well as homologous intracellular sequences across species suggests that the intracellular domains play a role in signal transduction. Indeed a cytoplasmic tailless mutant of muFc$_\gamma$RII$_1$ transfected into CHO cells was less capable of mediating internalization of opsonized *T. gondii* than the full length receptor (96). However, the relevance of *T. gondii* internalization to Fc$_\gamma$R-mediated phagocytosis in macrophages or neutrophils has come under question (98).

Analysis of second messengers and effectors involved in $Fc_\gamma R$ signaling has not been approached in an orderly fashion. Many studies involve simultaneous stimulation of multiple $Fc_\gamma R$ forms, and the type of ligand presented varies considerably between experiments. Also, investigators examining $Fc_\gamma R$-mediated functions use many different cell systems. Due to these variations, many conflicting results appear in the literature on $Fc_\gamma R$ signaling. The most consistent results are presented below.

The role of $Na^+$ in phospholipase $A_2$ activation upon binding of immune complexes to mouse peritoneal macrophages has been examined. There was a $Na^+$ requirement for phospholipase $A_2$ activation that could be replaced by an ionophore mediated $Ca^{2+}$ influx (99). Not only could $Ca^{2+}$ replace $Na^+$ in phospholipase $A_2$ activation upon immune complex binding but $Ca^{2+}$ was required, as shown by the inhibition of phospholipase $A_2$ activity in the presence of EGTA. Thus, the stimulation of phospholipase activity by $muFc_\gamma R$ may be a sequential event requiring a $Na^+$ influx followed by an increase in intracellular $Ca^{2+}$.

In contrast, several groups have shown that $Ca^{2+}$ is *not* an important signal for phagocytosis by neutrophils or macrophages (100). No rise in $[Ca^{2+}]_i$ was detected during phagocytosis, and depletion or buffering of $[Ca^{2+}]_i$ did not affect phagocytosis (101). However, protein kinase C activity and phosphoinositide turnover were enhanced in human neutrophil $Fc_\gamma R$-mediated phagocytosis (38). Phorbol esters, which are known to activate protein kinase C, also enhanced phagocytosis (102).

A flux in $[Ca^{2+}]_i$ is required for $O_2^{\cdot}$ production upon cross-linking of $huFc_\gamma RII$. Extensive cross-linking of $huFc_\gamma RII$ on IFN-$\gamma$ stimulated peripheral blood

monocytes and neutrophils, or IFN-γ differentiated U937 cells induced a rise in $[Ca^{2+}]_i$ associated with $O_2^{-\cdot}$ production (103). Addition of EGTA decreased the rise in $[Ca^{2+}]_i$ and $O_2^{-\cdot}$ production in IFN-γ primed neutrophils but did not affect IFN-γ activated U937 cells. The more transient rise in $[Ca^{2+}]_i$ of the U937 cells may be due to release of $Ca^{2+}$ solely from internal stores, whereas the more sustained $[Ca^{2+}]_i$ increase in neutrophils probably also requires influx of extracellular $Ca^{2+}$.

G proteins as well are probably involved in the neutrophil huFc$_\gamma$RII-mediated respiratory burst and lysosomal hydrolase release. Extensive cross-linking of neutrophils with the anti-huFc$_\gamma$RII mAb KuFc79 and anti-mouse F(ab')$_2$ triggered an oxidative burst and $O_2^{-\cdot}$ production (104). The Fc$_\gamma$RII-mediated production of $O_2^{-\cdot}$ was almost completely inhibited by pertussis toxin whereas release of lysosomal hydrolases was inhibited only 50%. These data suggest there are at least two pathways of signal transduction. In contrast, surfaces coated with IgG triggered neutrophil degranulation and $O_2^{-\cdot}$ production in a manner that was unaffected by pertussis or cholera toxin, but was inhibited by pretreatment of the neutrophils with phorbol myristate acetate (PMA) (105). PMA has been shown to interfere with G protein-protein kinase C interactions following activation of neutrophils by f-met-leu-phe (106). Perhaps similar interference by PMA occurs during activation of neutrophil Fc$_\gamma$Rs. Cross-linking of neutrophil huFc$_\gamma$RII by surface bound IgG was shown to augment neutrophil GTP binding and GTPase activity in a pertussis toxin independent manner (105). This indirect evidence suggests that a pertussis toxin and cholera toxin independent G protein is involved in human neutrophil $O_2^{-\cdot}$ production and degranulation.

A difference in $Fc_\gamma R$ binding to soluble complexes compared to ligand-coated surfaces could account for the stimulation of different G proteins. Alternative signaling through neutrophil $huFc_\gamma RIIIB$ or distinct signaling by the multiple forms of $huFc_\gamma RII$ on neutrophils could also account for involvement of more than one G protein in neutrophil $O_2^{\cdot-}$ production and degranulation.

**$Fc_\gamma$Receptors in Autoimmune Diseases**

$Fc_\gamma Rs$, which are central to immune defense, ironically may play a pathologic role in autoimmune diseases. In autoimmune diseases, autoantibodies directed against a variety of self antigens, as in systemic lupus erythematosus (SLE), or against specific proteins, such as in myasthenia gravis (107), autoimmune hemolytic anemia (108), and cyclic amegakaryocytic thrombocytopenia (7) have been identified. There is, particularly in SLE and Sjögren's syndrome, often a parallel defect in macrophage function, shown by a decreased clearance of autologous IgG sensitized erythrocytes (EIgG) (109). Analogously, peritoneal macrophages from most strains of autoimmune mice are markedly inhibited in the binding and phagocytosis of EIgG (110). The defect in macrophage $Fc_\gamma R$ function is not due to an intrinsic macrophage abnormality since macrophages cultured from bone marrow are normal (111).

One thesis for the paralysis of $Fc_\gamma R$ function in certain autoimmune diseases is that the $Fc_\gamma Rs$ are downregulated by binding and clearance of the abundant autoantibody-induced immune complexes. However, recent work by Boros et al. (1) suggests that the paralysis of $Fc_\gamma R$ function is primarily due to specific anti-$Fc_\gamma R$ Ig, and not to immune complexes *per se*. There were surprisingly high levels of anti-$Fc_\gamma R$

Ig in many strains of autoimmune mice. Approximately 2% of the total IgM in serum of old NZB mice bound to a muFc$_\gamma$RII affinity column. (Fc$_\gamma$Rs will not bind to the Fc domains of IgMs). Furthermore, anti-Fc$_\gamma$R IgM mAbs isolated from autoimmune mice inhibited binding of immune complexes to mouse macrophage Fc$_\gamma$Rs. Interestingly, peritoneal macrophages isolated from BXSB ♂ mice functioned normally even though these mice have a severe form of lupus. However, these BXSB ♂ mice also have no circulating anti-Fc$_\gamma$R Ig, thus strengthening the correlation between the presence of anti-Fc$_\gamma$R Ig and paralysis of Fc$_\gamma$R-mediated functions.

There are well documented examples of naturally occurring Ig directed against Fc$_\gamma$R in human patients as well. The NA1/NA2 allotypic system of huFc$_\gamma$RIIIB can elicit antibody leading to neutropenia in infants (45). There are also cases in which anti-Fc$_\gamma$RIII antibodies were found in sera from SLE patients (9). Further isolation and characterization of anti-Fc$_\gamma$R autoantibodies is necessary to understand their role in autoimmune diseases.

## II. High Level Expression of a Soluble Truncated Human Fc Receptor

### Introduction

A hallmark of autoimmune diseases is the production of antibodies directed against self antigens or autoantibodies. These antibodies may have a well-defined specificity, as in myasthenia gravis, or may recognize a broad array of antigens, as in systemic lupus erythematosus (SLE). Current opinion holds that T cell dysfunction may be the cause of autoantibody expression. Often a defect in macrophage function, particularly in SLE and Sjogren's disease, is seen as well (109). This macrophage dysfunction was assumed to be due to the high level of circulating immune complexes present in autoimmune diseases since macrophages cultivated from bone marrow functioned normally *in vitro* (112). However, recently autoantibodies specifically directed against $Fc_{\gamma}Rs$ have been isolated from the sera of both autoimmune mice and human autoimmune patients using a soluble mouse $Fc_{\gamma}RII$ (1). The presence of high titers of these anti-$Fc_{\gamma}R$ autoantibodies in some mice autoimmune strains correlated with previously reported macrophage dysfunction in those strains (110).

The possibility that anti-$Fc_{\gamma}R$ autoantibodies are the cause of macrophage dysfunction in human autoimmune diseases warrants further investigation. However, the soluble mouse $Fc_{\gamma}RII$ used in the initial studies may not be the best tool to detect anti-human $Fc_{\gamma}R$ autoantibodies. The human autoantibodies that were detected using the soluble $muFc_{\gamma}RII$ recognized only $huFc_{\gamma}RIII$ in cell staining experiments (113). The reason for this result is not clear since $muFc_{\gamma}RII$ has some homology to both $huFc_{\gamma}RII$ and $huFc_{\gamma}RIII$. Thus, a soluble human $Fc_{\gamma}RII$ would be useful in

determining if the specificity of human anti-$Fc_\gamma R$ autoantibodies is confined to $huFc_\gamma RIII$.

**Results**

Large quantities of receptor are needed to screen for and possibly purify anti-$Fc_\gamma R$ autoantibodies from autoimmune patients' sera. For this purpose, a putative $huFc_\gamma RII$ cDNA clone was obtained from Dr. Y. Kochan and sequenced (Fig. 1). The cDNA encoded the $huFc_\gamma RIIA$ isotype, which is the predominant $huFc_\gamma RII$ isotype on macrophages and neutrophils and is 95% homologous in its extracellular domain to other $huFc_\gamma RII$ isotypes. Due to this homology, any isotype would be suitable for screening purposes. Construction of a $huFc_\gamma RIIA$ cDNA lacking the putative transmembrane and cytoplasmic coding regions was needed to permit secretion of the translated protein for easy purification.

This truncated $huFc_\gamma RIIA$ cDNA was constructed by oligonucleotide primer-directed *in vitro* mutagenesis using the polymerase chain reaction (114) and subcloned into the pcEXV-3 mammalian expression vector. The truncated cDNA terminates at codon 179 (Fig. 1), which results in the loss of 9 extracellular domain residues as well as the putative transmembrane and cytoplasmic domains. Dihydrofolate reductase deficient ($DHFR^-$) CHO cells were cotransfected with a DHFR-minigene (pMG1) (115) and the subcloned $huFc_\gamma RIIA$ cDNA by the calcium phosphate-DNA coprecipitation method (116). Transfected CHO cells were selected in hypoxanthine-deficient media. Individual colonies were isolated and tested by PCR amplification of nuclear DNA for the presence of the truncated $huFc_\gamma RIIA$ cDNA.

```
-29                                                                    -5
MetSerGlnAsnValCysProArgAsnLeuTrpLeuLeuGlnProLeuThrValLeuLeuLeuLeuAlaSerAla
ATGTCTCAGAATGTATGTCCCAGAAACCTGTGGCTGCTTCAACCATTGACAGTTTTGCTGCTGCTGGCTTCTGCA

          -1 +1                                                        21
AspSerGlnAlaAlaProProLysAlaValLeuLysLeuGluProProTrpIleAsnValLeuGlnGluAspSer
GACAGTCAAGCTGCTCCCCCAAAGGCTGTGCTGAAACTTGAGCCCCCGTGGATCAACGTGCTCCAGGAGGACTCT

                                                                       46
ValThrLeuThrCysGlnGlyAlaArgSerProGluSerAspSerIleGlnTrpPheHisAsnGlyAsnLeuIle
GTGACTCTGACATGCCAGGGGGCTCGCAGCCCTGAGAGCGACTCCATTCAGTGGTTCCACAATGGGAATCTCATT

                                                                       71
ProThrHisThrGlnProSerTyrArgPheLysAlaAsnAsnAsnAspSerGlyGluTyrThrCysGlnThrAla
CCCACCCACACGCAGCCCAGCTACAGGTTCAAGGCCAACAACAATGACAGCGGGGAGTACACGTGCCAGACTGCC

                                                                       96
GlnThrSerLeuSerAspProValHisLeuThrValLeuSerGluTrpLeuValLeuGlnThrProHisLeuGlu
CAGACCAGCCTCAGCGACCCTGTGCATCTGACTGTGCTTTCCGAATGGCTGGTGCTCCAGACCCCTCACCTGGAG

                                                                      121
PheGlnGluGlyGluThrIleMetLeuArgCysHisSerTrpLysAspLysProleuValLysValThrPhePhe
TTCCAGGAGGGAGAAACCATCATGCTGAGGTGCCACAGCTGGAAGGACAAGCCTCTGGTCAAGGTCACATTCTTC

                                                                      146
GlnAsnGlyLysSerGlnLysPheSerHisLeuAspProThrPheSerIleProGlnAlaAsnHisSerHisSer
CAGAATGGAAAATCCCAGAAATTCTCCCATTTGGATCCCACCTTCTCCATCCCACAAGCAAACCACAGTCACAGT

                                                                      171
GlyAspTyrHisCysThrGlyAsnIleGlyTyrThrLeuPheSerSerLysProValThrIleThrValGlnVal
GGTGATTACCACTGCACAGGAAACATAGGCTACACGCTGTTCTCATCCAAGCCTGTGACCATCACTGTCCAAGTG

                                                                      196
ProSerMetGlySerSerSerProMetGlyIleIleValAlaValValIleAlaThrAlaValAlaAlaIleVal
CCCAGCATGGGCAGCTCTTCACCAATGGGGATCATTGTGGCTGTGGTCATTGCGACTGCTGTAGCAGCCATTGTT

                                                                      221
AlaAlaValValAlaLeuIleTyrCysArgLysLysArgIleSerAlaAsnSerThrAspProValLysAlaAla
GCTGCTGTAGTGGCCTTGATCTACTGCAGGAAAAAGCGGATTTCAGCCAATTCCACTGATCCTGTGAAGGCTGCC

                                                                      246
GlnPheGluProProGlyArgGlnMetIleAlaIleArgLysArgGlnLeuGluGluThrAsnAsnAspTyrGlu
CAATTTGAGCCACCTGGACGTCAAATGATTGCCATCAGAAAGAGACAACTTGAAGAAACCAACAATGACTATGAA

                                                                      271
ThrAlaAspGlyGlyTyrMetThrLeuAsnProArgAlaProThrAspLysProLeuValLysValThrPhePhe
ACAGCTGACGGCGGCTACATGACTCTGAACCCCAGGGCACCTACTGACGATGATAAAAACATCTACCTGACTCTT

                                  281
ProProAsnAspHisValAsnSerAsnAsnEnd
CCTCCCAACGACCATGTCAACAGTAATAACTAA
```

Fig. 1. HuFc$_\gamma$RIIA sequence. The putative signal sequence is overlined, and the transmembrane sequence is underlined. The first codon of the mature protein is numbered +1.

HuFc$_\gamma$RIIA cDNA-containing clones were grown in increasing concentrations of methotrexate to amplify huFc$_\gamma$RIIA gene expression.

Clones of cells that proliferated in the presence of 2.0 $\mu$M methotrexate were screened for secretion of soluble huFc$_\gamma$RIIA by a binding inhibition assay. Suspensions of cells expressing membrane bound huFc$_\gamma$RIIA were incubated with mAb IV.3, an anti-Fc$_\gamma$RII mouse mAb, in the presence of conditioned media (concentrated 10-fold) from methotrexate-amplified clones. The cells were then gently washed by centrifugation and resuspended in FITC-conjugated goat anti-mouse IgG F(ab')$_2$. After extensive washing, cell fluorescence was measured on a Coulter Epics Cell Sorter with a 3 decade log fluorescence scale (Fig. 2). Conditioned media from several transfectants containing the truncated huFc$_\gamma$RIIA cDNA, as determined by PCR amplification, blocked mAb IV.3 binding. Subsequent titration experiments identified conditioned media from the CT14 clone as the most potent inhibitor of mAb IV.3 binding.

Soluble huFc$_\gamma$RIIA protein was partially purified from CT14 supernatant by human IgG-sepharose affinity chromatography (Fig. 3A), which naturally necessitates that the secreted protein be active. The major protein in the eluted fractions, as visualized by SDS-PAGE, had a $M_r$ of ~ 27 kDa (Fig. 3B). The receptor is probably glycosylated, as was the truncated soluble muFc$_\gamma$RII, on both potential N-linked glycosylation sites since the predicted weight of the 179 amino acid soluble huFc$_\gamma$RIIA is 20 kDa. (The soluble receptor was further purified by size on a Superdex-75 column). Identification of the purified receptor was confirmed by an ELISA utilizing

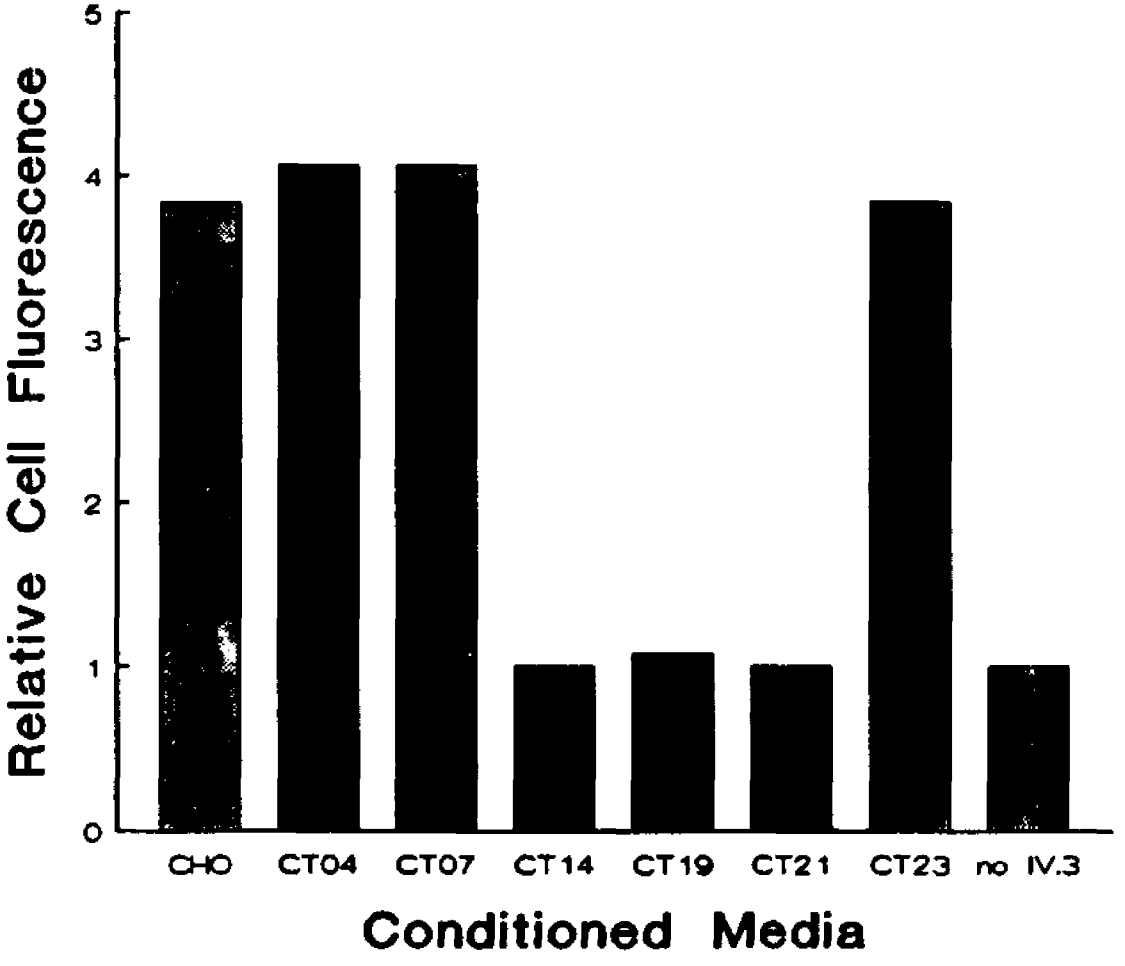


**Fig. 2.** Binding inhibition assay. Conditioned media of CHO clones transfected with a cDNA encoding a secretable huFc$_\gamma$RIIA were tested for their ability to block the binding of mAb IV.3 Fab, an anti-huFc$_\gamma$RII mAb, to cells expressing membrane bound huFc$_\gamma$RIIA. Medium collected from untransfected CHO cells was used to determine maximal cell staining (CHO). Background cell fluorescence was determined by omitting mAb IV.3 (no IV.3).

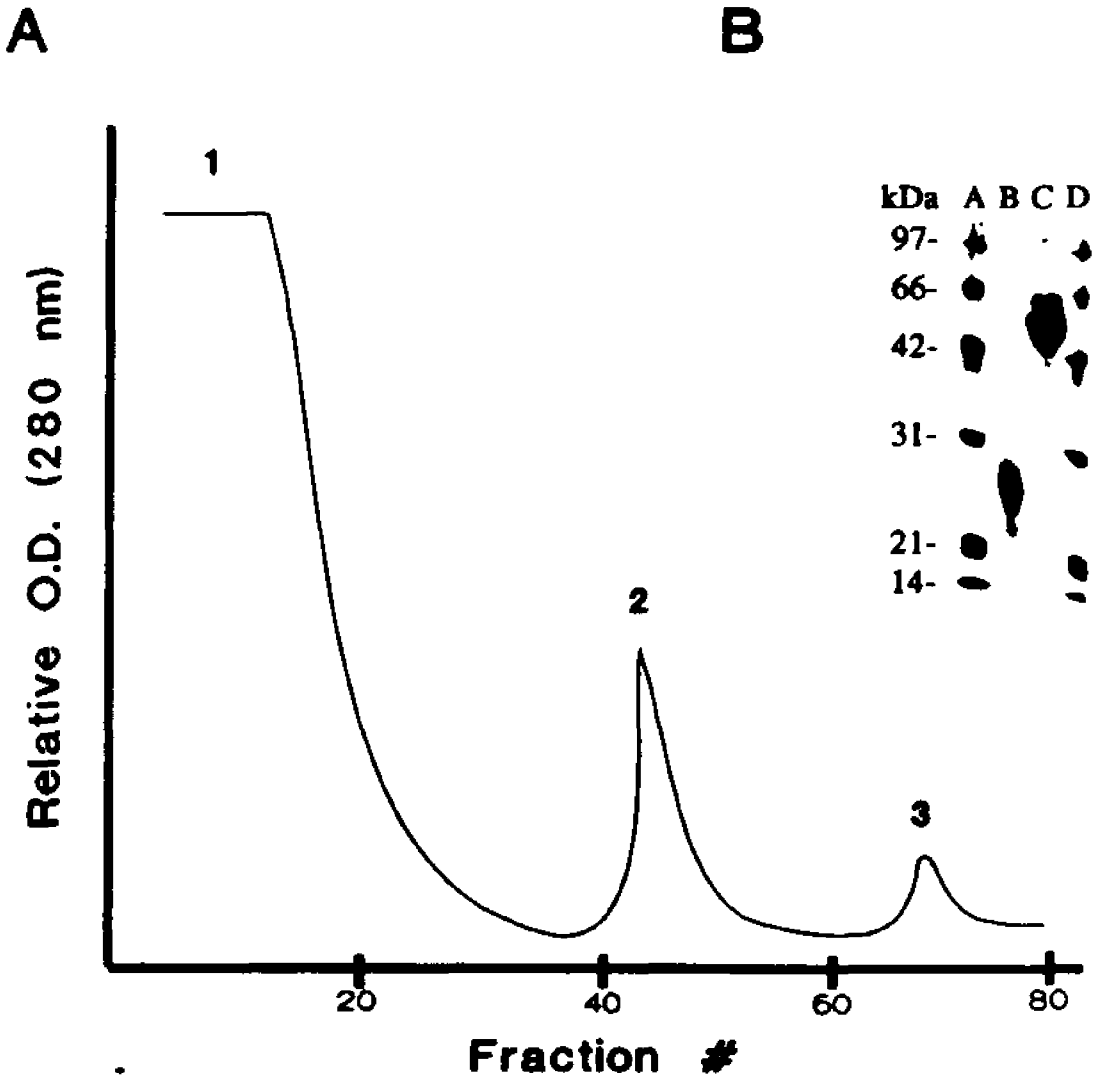


Fig. 3. Purification of soluble huFc$\gamma$RIIA. (A) Human IgG-Sepharose affinity chromatography. Ten-fold concentrated conditioned media from CT14 cells, dialyzed against 10 mM sodium phosphate buffer, pH 7.0, was passed over a huIgG-Sepharose column (peak 1) and washed with 10 mM sodium phosphate buffer, 0.15 M NaCl, pH 7.0 (peak 2). Bound proteins were eluted in 0.10 M sodium acetate buffer, 0.5 M NaCl, pH 4.0 (peak 3). (B) SDS-PAGE of eluted proteins. Molecular weight standards were loaded into lanes A & D. A fraction from peak 3 was loaded into lane B, and a fraction from peak 2 was loaded into lane C.

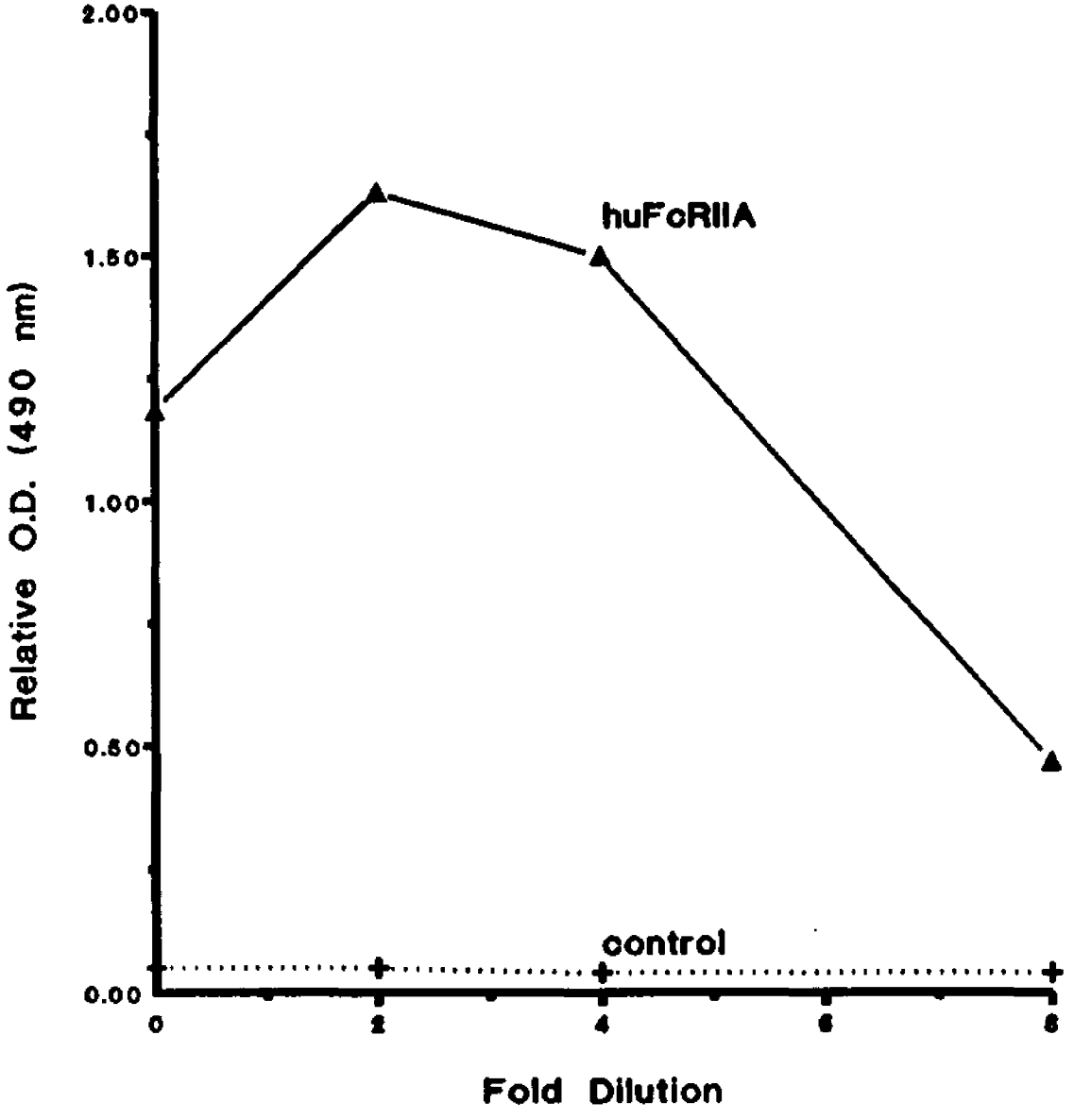


**Fig. 4.** Elisa for huFc$_\gamma$RIIA. Plastic wells were coated with purified, soluble huFc$_\gamma$RIIA protein (5 $\mu$g/ml) and multiple two-fold dilutions and then blocked with 1% BSA. Control wells were coated with only 1% BSA. The wells were then incubated sequentially with mAb IV.3 Fab, an anti-Fc$_\gamma$RII mouse mAb, and biotinylated goat anti-mouse IgG F(ab')$_2$. The amount of reactivity was quantified in a colorimetric assay utilizing avidin-conjugated horseradish peroxidase.

mAb IV.3 Fab (Fig. 4). From one liter of cultured CT14 media, approximately 1-2 mg of receptor was purified.

In collaboration with Dr. P. Boros, an ELISA was established to screen autoimmune sera from patients suffering from Sjoren's syndrome, systemic lupus erythematosus, or progressive systemic sclerosis for anti-huFc$_\gamma$RIIA autoantibodies. In a preliminary screening, eleven of twenty-six sera reacted with the soluble huFc$_\gamma$RIIA (Appendix Fig. A). Of these eleven, six also reacted with the soluble muFc$_\gamma$RII, whereas five of the twenty-six reacted only with muFc$_\gamma$RII. Thus, the soluble huFc$_\gamma$RIIA detected autoantibodies that went undetected by the soluble muFc$_\gamma$RII.

**Discussion**

Earlier studies utilizing a soluble muFc$_\gamma$RII protein detected significant levels of anti-Fc$_\gamma$R autoantibodies in the sera of patients suffering from various autoimmune diseases (1). It was postulated that these autoantibodies may play a role in the macrophage dysfunction observed in these patients. For unknown reasons, in cell staining experiments, the autoantibodies identified using the soluble muFc$_\gamma$RII recognized only huFc$_\gamma$RIII and not huFc$_\gamma$RII. To identify any anti-huFc$_\gamma$RII autoantibodies that had gone undetected, large quantities of huFc$_\gamma$RII were needed to rescreen patients' sera.

Using PCR-directed mutagenesis, a cDNA encoding a soluble form of huFc$_\gamma$RIIA was created by deleting its transmembrane and cytoplasmic domains. High levels of active protein were purified from cultured media of CHO cells transfected

with the truncated cDNA. The identity of the purified receptor was confirmed by binding to mAb IV.3, an anti-huFc$_\gamma$RII mAb. By using this purified receptor in an ELISA, high levels of anti-huFc$_\gamma$RIIA autoantibodies were detected in 24% of autoimmune patients' sera. In 50% of these patients, high levels of anti-muFc$_\gamma$RII autoantibodies were detected, and 20% had both anti-huFc$_\gamma$RII and anti-muFc$_\gamma$RII autoantibodies. The presence of one type of autoantibody seems slightly to predispose the patient for expression of the other autoantibody. Understanding of any pathogenicity of these autoantibodies must await their purification and analysis. Preliminary studies indicate that the anti-muFc$_\gamma$RII autoantibodies activate neutrophil degranulation (113) and may stimulate cytokine secretion by macrophages *in vivo* (P. Boros *et al.*, unpublished results).

The rapid growth of CT14 cells and the relative ease of purifying high levels of active, soluble huFc$_\gamma$RIIA makes possible many other uses for this protein. For example, structural studies of crystallized, soluble huFc$_\gamma$RIIA by x-ray diffraction are feasible. Analysis of crystals formed from glycosylated, soluble muFc$_\gamma$RII have been hampered by excessive heterogeneity in the crystal structure (Z. Qu, personal communication). The human receptor has only two potential N-linked glycosylation sites as opposed to four in the mouse receptor and thus, may be more suitable for crystallization. Detailed structural information would increase our understanding of the nature of IgG-Fc$_\gamma$R binding and possibly of intermolecular interactions between Fc$_\gamma$Rs.

Models for neutrophil, GPI-anchored huFc$_\gamma$RIII-2 function have been proposed in which interaction with huFc$_\gamma$RII is required to transduce an activation signal to the

cell interior. Establishing that soluble $Fc_\gamma Rs$ interact in solution, while not direct evidence, would give credence to this hypothesis. Preliminary studies show that soluble $muFc_\gamma RII$ interact transiently in solution (Qu *et al.*, unpublished results). Similar studies are planned utilizing soluble $huFc_\gamma RIIA$ alone and in combination with soluble $muFc_\gamma RII$.

**Materials and Methods**

*PCR amplification and subcloning*

A truncated $huFc_\gamma RIIA$ cDNA was constructed by oligonucleotide primer-directed *in vitro* mutagenesis using the polymerase chain reaction (114). The 17-mer antisense primer encoded a nonsense mutation in codon 179. The sense primer corresponded to a segment of the T7 promoter sequence of pGEM-4, in which the $huFc_\gamma RIIA$ cDNA was subcloned. For sequence amplification, 8 $\mu$g/ml of template and 50 pM primers were heated to 94°C for 1 min, allowed to reanneal at 50°C for 2 min, and then incubated at 72°C for 3 min in the presence of 4 U/ml of Taq polymerase (Promega Co., Madison, WI) and 500 $\mu$M dNTPs for 35 cycles. The ends of the gel purified product were filled in by treatment with Klenow (New England Biolabs, Inc., Beverly, MA) and then treated with T4 DNA kinase (New England Biolabs, Inc.) (117) prior to subcloning into the Sma I site of pcEXV-3 (118). pcEXV-3 is a mammalian gene expression vector with an SV-40 early gene promoter and polyadenylation signal. Competent bacteria were transformed with the ligation product (117). Multiple colonies were identified which contained the desired plasmid. A plasmid containing the truncated $huFc_\gamma RIIA$ cDNA in the correct orientation for

expression was fully sequenced on both strands on an Applied Biosystems Model 373A Sequencer (Mount Sinai Medical Center, DNA Core Facility) to confirm the deletion mutation. The truncated cDNA was isolated by EcoR I digestion of the plasmid and resubcloned (117) into the EcoR I site of pcEXV-3 in order to eliminate pGEM-4 sequences from the 5' end of the cDNA. Again, competent bacteria were transformed, and plasmids containing huFc$_\gamma$RIIA in the correct orientation were isolated.

*Expression in DHFR$^-$ CHO cells.*

DHFR$^-$ CHO cells (115) were transfected with 1 $\mu$g/ml of a DHFR-minigene (pMG1) (115) with and without 18 $\mu$g/ml of the subcloned huFc$_\gamma$RIIA cDNA by the calcium phosphate-DNA coprecipitation method (116). Transfected CHO cells were selected in hypoxanthine-deficient DME supplemented with 10% dialyzed FCS, 16 $\mu$M thymidine, and 300 $\mu$M proline. Individual colonies were isolated and tested by PCR amplification of extracted nuclear DNA for the presence of the huFc$_\gamma$RIIA cDNA. HuFc$_\gamma$RIIA cDNA-containing clones and control transfectants were grown in slowly increasing concentrations of methotrexate (Sigma Chemical Co., St. Louis, MO), from 0.02 to 2.0 $\mu$M, to amplify huFc$_\gamma$RIIA gene expression. Collected supernatants were centrifuged to remove cells and debris.

Suspensions of CHO cells expressing membrane bound huFc$_\gamma$RIIA (C-FcRIIA) were incubated with the collected supernatants in the presence of 0.5 $\mu$g/ml of mAb IV.3 (Mederex Inc., Hanover, NH). The cells were then gently washed by centrifugation and resuspended in 20 $\mu$g/ml of FITC-conjugated goat anti-mouse IgG F(ab')$_2$ (Organon Teknika-Cappel, Inc., West Chester, PA). After extensive washing,

cell fluorescence was measured on a Coulter Epics Cell Sorter with a 3 decade log fluorescence scale. Supernatants were subsequently titrated and assayed again to identify the one with the greatest inhibitory potential.

*Purification of truncated soluble huFc$_\gamma$RIIA*

CT14 conditioned media was centrifuged to remove cells and debris and dialyzed against 10 mM sodium phosphate, pH 7.0. The dialyzed media was concentrated ten-fold by pressure filtration in an Amicon centriprep-10 concentrator with a MW cut off at 10 kDa. The concentrated media was passed over a human IgG-sepharose column. The column was washed with 10 mM sodium phosphate, 150 mM NaCl, pH 7.0, and bound proteins were eluted with 100 mM sodium acetate, 500 mM NaCl, pH 4.0. The eluted proteins were again dialyzed against 10 mM sodium phosphate, pH 7.0. The soluble receptor was further purified by size on a Superdex 75 column. The purity and size of the eluted protein(s) was determined by SDS-PAGE as described previously (119).

*ELISA to identify soluble huFc$_\gamma$RII*

Identification of the purified receptor was confirmed by an ELISA in which wells were coated with 5 $\mu$g/ml of the purified receptor and blocked with 1% BSA. Between washings, 2 $\mu$g/ml of mAb IV.3 Fab was added followed by 10 $\mu$g/ml of biotinylated goat anti-mouse IgG F(ab')$_2$. After extensive washing, the reaction was developed with avidin-peroxidase as described previously (51).

## III. Regulation of Phagocytosis and $[Ca^{2+}]_i$ Flux by Distinct Regions of an Fc Receptor

### Introduction

Fc receptors for IgG ($Fc_\gamma R$) provide a key link between humoral and cell-mediated immune responses. Activation of FcRs, which are univalent, requires cross-linking of multiple receptors by multivalent immune complexes. The responses of neutrophils and macrophages to the binding of immune complexes include phagocytosis, the production of oxidative metabolites, antibody-dependent cell-mediated cytotoxicity (ADCC), and the production and release of inflammatory mediators. Human $Fc_\gamma Rs$ belong to a multi-gene family divided into three subclasses based on differences in structure and avidity for IgG: $huFc_\gamma RI$, $huFc_\gamma RII$, and $huFc_\gamma RIII$. Within a $huFc_\gamma R$ subclass, receptors have nearly identical extracellular domains but differ in their intracellular domains. These differences may account for variations in cell activation among $huFc_\gamma Rs$ (2) and suggest that the intracellular domains play a role in signal transduction. An individual receptor form can trigger multiple cellular responses, and those responses utilize different signal transduction pathways. For example, the oxidative burst mediated by $huFc_\gamma RII$ on macrophages requires a rapid increase in $[Ca^{2+}]_i$ (103); however, blocking this increase does not inhibit $huFc_\gamma RII$-mediated phagocytosis (101). At some point a bifurcation of the signal pathway must occur. How these dual signal pathways are activated by $huFc_\gamma RII$ is not clear since Fc receptors have no enzyme activity, nor do they resemble structurally G protein-coupled receptors.

To identify intracellular regions required for signaling, I transfected cDNAs encoding a human Fc receptor, huFc$_\gamma$RIIA (36), and a series of truncated huFc$_\gamma$RIIA into P388D$_1$ cells, a mouse macrophage-like cell line, and into CHO cells, a hamster fibroblast cell line. Studies of mRNA levels (36) have shown that huFc$_\gamma$RIIA is the predominant Fc$_\gamma$RII on neutrophils, macrophages, and platelets. The cytoplasmic domain of huFc$_\gamma$RIIA has some homology to muFc$_\gamma$RII$_2$, which is expressed on P388D$_1$ cells. CHO cells do not express any native Fc$_\gamma$R and thus provide a control for the cell specificity of huFc$_\gamma$RIIA-mediated functions in P388D$_1$ cells.

**Results**

In the cytoplasmic domains of huFc$_\gamma$RIIA and muFc$_\gamma$RII$_2$, two negatively charged regions and intervening tyrosine and leucine residues are conserved (Fig. 5). Nonsense mutations in the 3′ end of a huFc$_\gamma$RIIA cDNA clone were introduced by cDNA amplification using polymerase chain reaction (PCR) antisense primers containing the desired nucleotide alteration (114). Three mutants that encode proteins with truncated COOH termini were prepared (Fig. 5). The most extensive truncation of huFc$_\gamma$RIIA, Δ207, had all but two putative cytoplasmic amino acid residues eliminated. The second, Δ233, and third, Δ264, truncations retained, respectively, 28 and 59 residues of the 76 amino acid cytoplasmic domain. Δ233 terminates before the first charged amino acid stretch, and Δ264 terminates after the second.

The wild-type and truncated cDNAs were subcloned into the pcEXV-3 mammalian expression vector (118) and then transfected into CHO and P388D$_1$ cells by the calcium-phosphate coprecipitation method (116). To transfect P388D$_1$ cells,

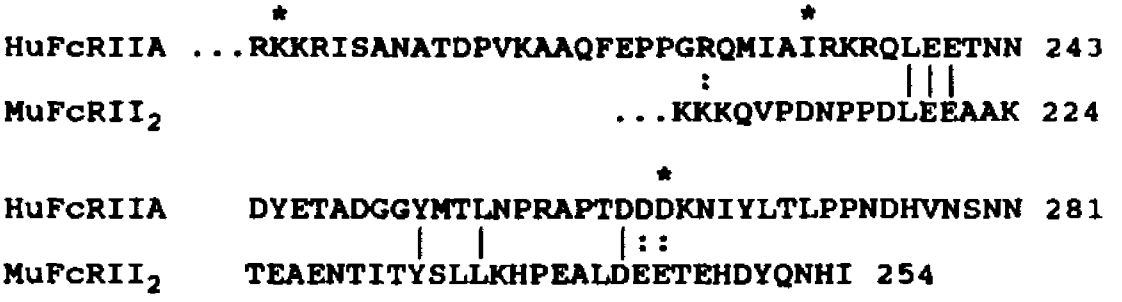


**Fig. 5.** Alignment of $Fc_{\gamma}R$ sequences. Identical residues are joined by solid lines, and homologous residues by dashed lines. Asterisks (*) are placed over the new terminal amino acids of the truncated $huFc_{\gamma}RIIA$.

chloroquine was added to the transfection media. $P388D_1$ transfectants expressing wild-type $huFc_\gamma RIIA$ (P-FcRIIA) were identified by their ability to bind mAb IV.3 Fab, an anti-$huFc_\gamma RII$ mouse mAb, in comparison to mock transfected $P388D_1$ cells (P-NEG) (Fig. 6A&B). Likewise, CHO transfectants expressing wild-type $huFc_\gamma RIIA$ (C-FcRIIA) were compared to mock transfected CHO cells (C-NEG) (Fig. 6C&D). There was no significant binding to $huFc_\gamma RIIA$-expressing cells by an isotype control mAb. Mutant $huFc_\gamma RIIA$-expressing transfectants were similarly identified.

The $P388D_1$ cell line expresses approximately $3x10^5$ $muFc_\gamma RII$ and $muFc_\gamma RIII$ per cell (120). Scatchard analyses of direct binding assays using $^{125}I$-labeled mAb IV.3 were done for one CHO transfectant and for one $P388D_1$ transfectant (Fig. 7). The level of $huFc_\gamma RIIA$ expression on the other $P388D_1$ and CHO transfectants was determined by comparative fluorescence according to cell type. For transfectants utilized in subsequent experiments, expression levels varied between $3.1x10^5$- $6.0x10^5$ receptors per cell for CHO transfectants and between $6.8x10^5$- $9.0x10^5$ for $P388D_1$ transfectants.

Internalization of antibody-$Fc_\gamma R$ (Ab-$Fc_\gamma R$) complexes was assayed by coating cell suspensions with mAb IV.3 Fab at 4°C and then cross-linking the Fab with goat $F(ab')_2$ antibody to mouse IgG. After incubation at 37°C to allow the cells to internalize receptor-bound complexes, the cells were returned to 4°C and assayed by flow cytometry for complexes remaining on the cell surface (Fig. 8). Typically, for P-FcRIIA cells, > 70% of the $huFc_\gamma RII$-specific complexes were rapidly internalized, with a plateau after 10 min. Similar results were obtained when the native $muFc_\gamma Rs$

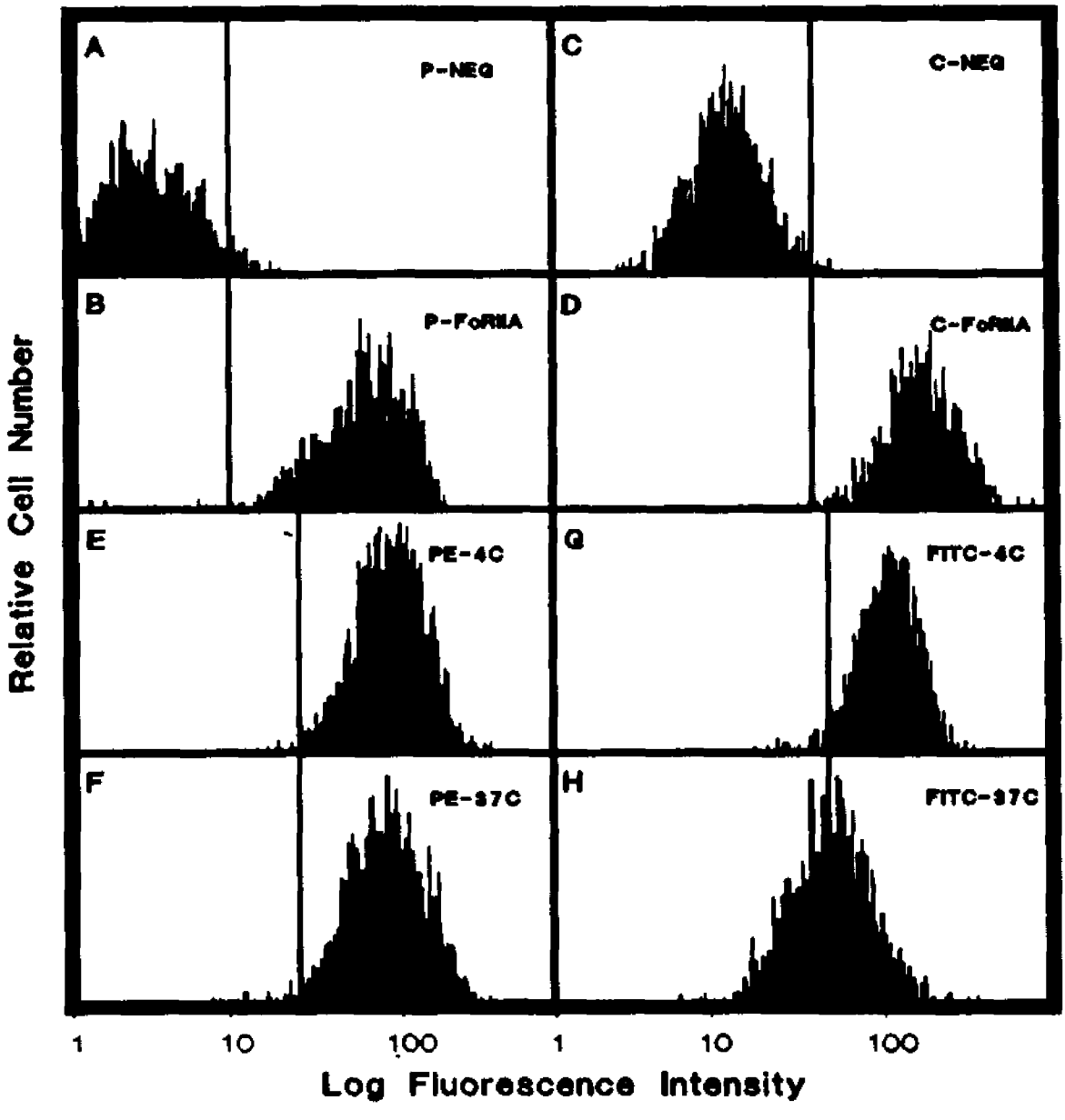


Fig. 6. (A-D) Transfectant screening. Negative control and huFc$_\gamma$RIIA transfected P388D$_1$ (A&B) and CHO (C&D) clones were incubated at 4°C with mAb IV.3, followed by FITC-goat anti-mouse IgG F(ab')$_2$. After extensive washing cell fluorescence was measured by a Coulter Epics Cell Sorter with a 3 decade log fluorescence scale. (E-H) Receptor internalization. P-FcRIIA cells were labeled with mAb IV.3 Fab followed by either phycoerythrin (PE)-conjugated (E&F) or fluorescein isothiocyanate (FITC)-conjugated (G&H) goat anti-mouse IgG F(ab')$_2$. The cells were then incubated either at 4°C or 37°C for 15 min prior to washing and fluorescence analysis.

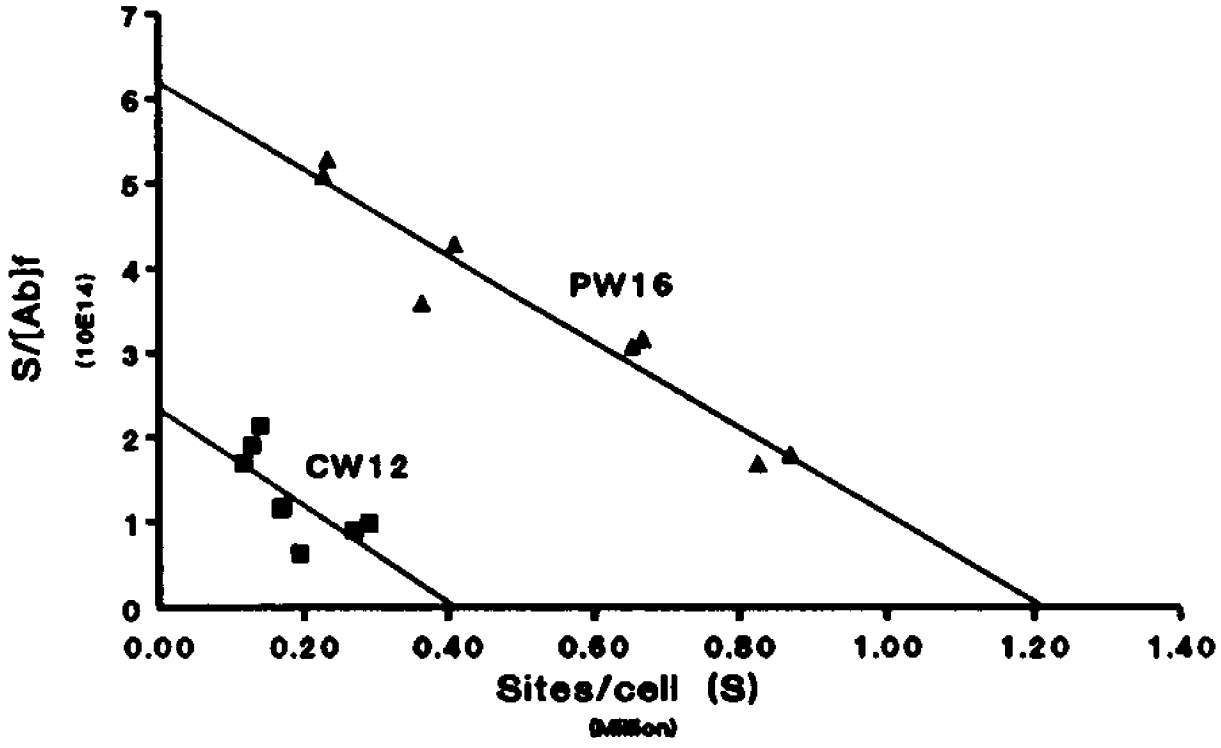


Fig. 7. Scatchard analysis. The number of huFc$_\gamma$RIIA per cell for a huFc$_\gamma$RIIA-expressing P388D$_1$ clone (A: PW16) and a CHO clone (B: C-FcRIIA) was calculated following a direct binding assay utilizing various non-saturating concentrations of $^{125}$I-mAb IV.3 and 2.5x10$^6$ cells/ml.

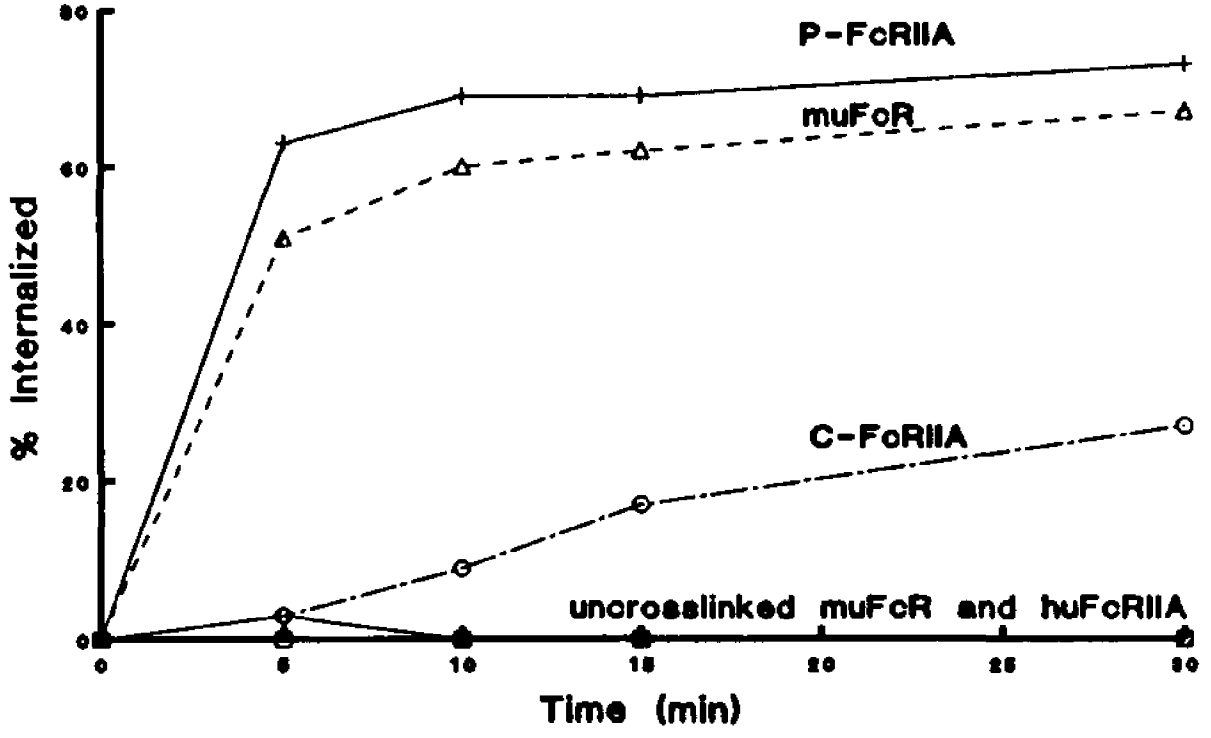


Fig. 8. Time course of internalization. Internalization of antibody cross-linked huFc$_\gamma$RIIA in suspensions of P-FcRIIA (-+-) or C-FcRIIA (-O-) cells incubated at 37°C is compared to internalization of antibody cross-linked native muFc$_\gamma$R on P-FcRIIA cells (-Δ-). In the other two samples, after cross-linking either the native mouse Fc$_\gamma$R (-□-) or huFc$_\gamma$RIIA (-◇-) and incubating the cells at 37°C, the *uncross-linked* receptor type was stained at 4°C. All experiments were repeated on at least three separate days. A representative experiment is shown.

were labeled with mAb 2.4G2 (120), a rat antibody specific for muFc$_\gamma$RII and muFc$_\gamma$RIII, and cross-linked with a goat F(ab')$_2$ antibody to rat IgG. Internalization of either human or mouse Fc$_\gamma$Rs did not affect the other. In contrast to the P-FcRIIA cells, C-FcRIIA cells internalized huFc$_\gamma$RIIA-specific complexes only at a slow steady rate; < 30% of the complexes were internalized after 30 min. The initial rate of internalization in P-Fc$_\gamma$RIIA cells was 18 times that of C-Fc$_\gamma$RIIA cells.

Loss of huFc$_\gamma$RIIA from the surface was due to internalization and not shedding, because total cell bound counts remained constant before (1968$\pm$267) and after (1929$\pm$335) a 15 min incubation of P-FcRIIA cells at 37°C with $^{125}$I-labeled complexes. Likewise, P-FcRIIA cells incubated at 4°C or 37°C for 15 min with phycoerythrin (PE)-conjugated complexes had no significant difference in fluorescence (Fig. 6E&F). Phycoerythrin fluorescence is unaffected by cellular internalization (121). Cell fluorescence was reduced 50% when P-FcRIIA cells were incubated at 37°C with complexes labeled with fluorescein (Fig. 6H&G), which is quenched in acidic cellular compartments (121,122). Internalization of the Ab-huFc$_\gamma$RIIA complexes was inhibited > 80% at 23°C compared to 37°C in P-FcRIIA cells, but internalization in C-FcRIIA cells was not markedly changed (Table 2). Thus, in regard to delivery to intracellular, low pH phagosomes and temperature sensitivity, the internalization of Ab-Fc$_\gamma$R complexes by P-FcRIIA cells mirrors macrophage phagocytosis of opsonized particles (123). The internalization in C-FcRIIA cells may be due to activation of a slow, temperature insensitive endocytic process common to all cells (123). In addition, macrophage phagocytosis specifically mediated by huFc$_\gamma$RII probably requires protein

**Table 2.** Regulation of internalization by huFc$_\gamma$RIIA. The ability of huFc$_\gamma$RIIA transfectants to internalize Ab-huFc$_\gamma$RIIA complexes during a 15 min incubation at 23°C versus 37°C was determined. The effects of calphostin C, genistein, and BAPTA-AM on a 15 min internalization at 37°C were also determined. The percentage of transfected cells that internalized at least one E-IV.3 Fab during a 20 min incubation at 37°C is compared to BAPTA-AM treated P-FcRIIA cells. Inhibitors were incubated with the cells for 30 min at 37°C and also included throughout the internalization procedure. Data are the mean internalization percentages (±SEM) of at least three independent experiments.

| | Transfected Cell Line | | |
|---|---|---|---|
| Internalization Conditions | P-FcRIIA | P-Δ264 | C-FcRIIA |
| | Internalization (%) | | |
| Ab-huFc$_\gamma$RIIA Complexes | | | |
| Control 37°C | 72±7 | 66±9 | 20±15 |
| 23°C | 11±1 | 9±3 | 14±1 |
| Calphostin C | 29±18 | 39±14 | - |
| Genistein | 32±8 | 18±14 | - |
| BAPTA-AM | 68±4 | - | - |
| E-IV.3 Fab | | | |
| Control | 30±2 | 1±1 | 0 |
| BAPTA-AM | 5±4 | - | - |

kinase C (PKC) (124,125) and tyrosine kinase(s) activation (126). Treatment of P-FcRIIA cells for at least 20 min with a PKC inhibitor (calphostin C) or a tyrosine kinase inhibitor (genistein) blocked internalization of Ab-huFc$_\gamma$RIIA complexes (Table 2). At the inhibitor concentration used, cell viability (trypan blue exclusion) was > 85%, and huFc$_\gamma$RIIA expression in control P-FcRIIA cells was unaffected by either inhibitor.

We examined huFc$_\gamma$RIIA-mediated internalization of opsonized particles by incubating the transfectants with mAb IV.3 Fab coated erythrocytes (E-IV.3 Fab) for 20 min at 37°C. Although P-FcRIIA and C-FcRIIA (wild type) cells were both able to rosette E-IV.3 Fab, only P-FcRIIA cells were able to internalize the opsonized erythrocytes (Table 2). The average percentage of P-FcRIIA cells that internalized at least one E-IV.3 Fab was 30±2. Neither cell type bound or internalized uncoated erythrocytes, nor did mock transfected P388D$_1$ cells bind or internalize E-IV.3 Fab (Fig 9). In both phagocytic assays, huFc$_\gamma$RIIA-mediated internalization was dependent on factors expressed in the macrophage cell line, P388D$_1$, but not found in the fibroblast cell line, CHO.

In order to determine which regions of huFc$_\gamma$RIIA are required for phagocytosis, transfected cells expressing truncated huFc$_\gamma$RIIA proteins were analyzed for both the internalization of Ab-huFc$_\gamma$RIIA complexes and of E-IV.3 Fab. The level of E-IV.3 Fab internalization was normalized relative to the internalization of positive control erythrocytes coated with rabbit IgG (EA) by each P388D$_1$ transfectant to compensate for possible differences due to the varying number of huFc$_\gamma$RIIA per cell

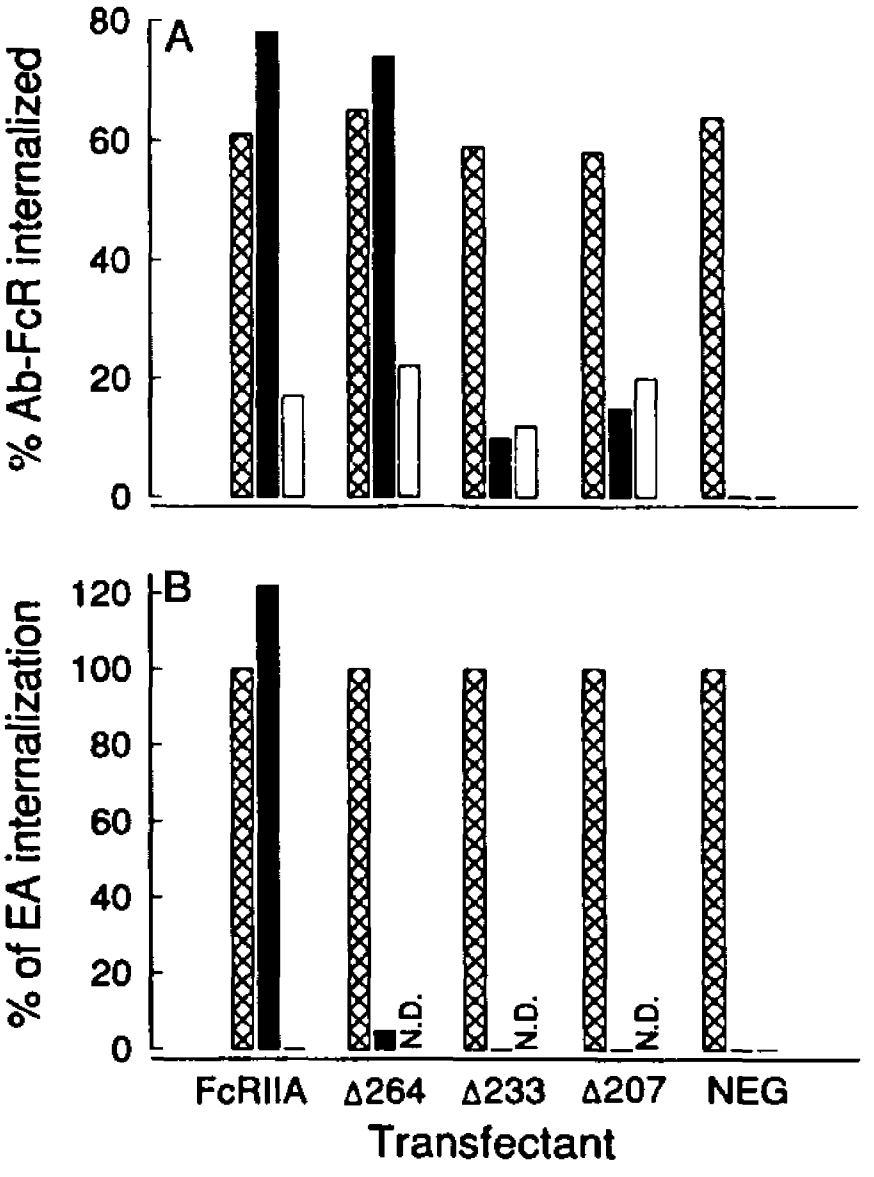


**Fig. 9.** HuFc$_\gamma$RIIA-mediated phagocytosis. **(A)** The percent internalization of huFc$_\gamma$RII-specific antibody complexes by each P388D$_1$ **(black)** and CHO **(open)** transfectant is shown. The percentage of bound muFc$_\gamma$R-specific antibody complexes internalized by each P388D$_1$ transfectant is shown as a positive control **(hatched)**. Experiments were repeated on at least three separate days. Representative experiments are shown. **(B)** The internalization of mAb IV.3 Fab coated erythrocytes (E-IV.3 Fab) by P388D$_1$ **(black)** and CHO **(open)** transfectants was normalized relative to the internalization of positive control erythrocytes, coated with rabbit antibody to erythrocytes (EA), by the corresponding P388D$_1$ transfectant. EA internalization was defined as 100% **(hatched)**.The mean values of three independent experiments are shown. (N.D.= not done).

among the transfectants. The Fc domain of rabbit IgG will bind to huFc$_\gamma$RII and muFc$_\gamma$R (2). P388D$_1$ cells transfected with the two shorter truncated receptors (P-Δ207 and P-Δ233) internalized < 20% of the Ab-huFc$_\gamma$RIIA complexes and no E-IV.3 Fab (Fig. 9). P-Δ264 cells internalized Ab-huFc$_\gamma$RIIA complexes as efficiently as cells expressing the wild-type receptor, P-FcRIIA. As in P-FcRIIA cells, internalization of Ab-huFc$_\gamma$RIIA complexes in P-Δ264 cells was highly temperature sensitive and blocked by PKC and tyrosine kinase inhibitors (Table 2). In contrast, E-IV.3 Fab were not internalized by P-Δ264 cells. Since all P388D$_1$ transfectants internalized muFc$_\gamma$R-specific antibody complexes and EA (Fig. 9), the phagocytic apparatus per se in each P388D$_1$ transfectant is functional. None of the CHO transfectants could efficiently internalize the Ab-huFc$_\gamma$RIIA complexes or opsonized erythrocytes, though they could avidly bind these particles. Thus, the phagocytosis of small antibody complexes, although similar to the phagocytosis of opsonized erythrocytes in its macrophage specificity, did not require the 17 terminal amino acids of huFc$_\gamma$RIIA.

The oxidative burst initiated by huFc$_\gamma$RII cross-linking on macrophages reportedly requires a rapid increase in $[Ca^{2+}]_i$ released from intracellular stores (103). To detect changes in $[Ca^{2+}]_i$ in huFc$_\gamma$RIIA transfected cells, we loaded the cells with indo-1-AM (a calcium fluorophore) (127). HuFc$_\gamma$RIIA sites were saturated with mAb IV.3 Fab, and cross-linked with goat F(ab')$_2$ antibody to mouse IgG at 37°C (128) (Fig. 10). The P-FcRIIA transfectant had an immediate flux in $[Ca^{2+}]_i$, which increased by 320±82 nM (mean±SEM) before returning to a baseline level of 102±20 nM. Neither mAb IV.3 Fab nor goat anti-mouse IgG F(ab')$_2$ alone could trigger this

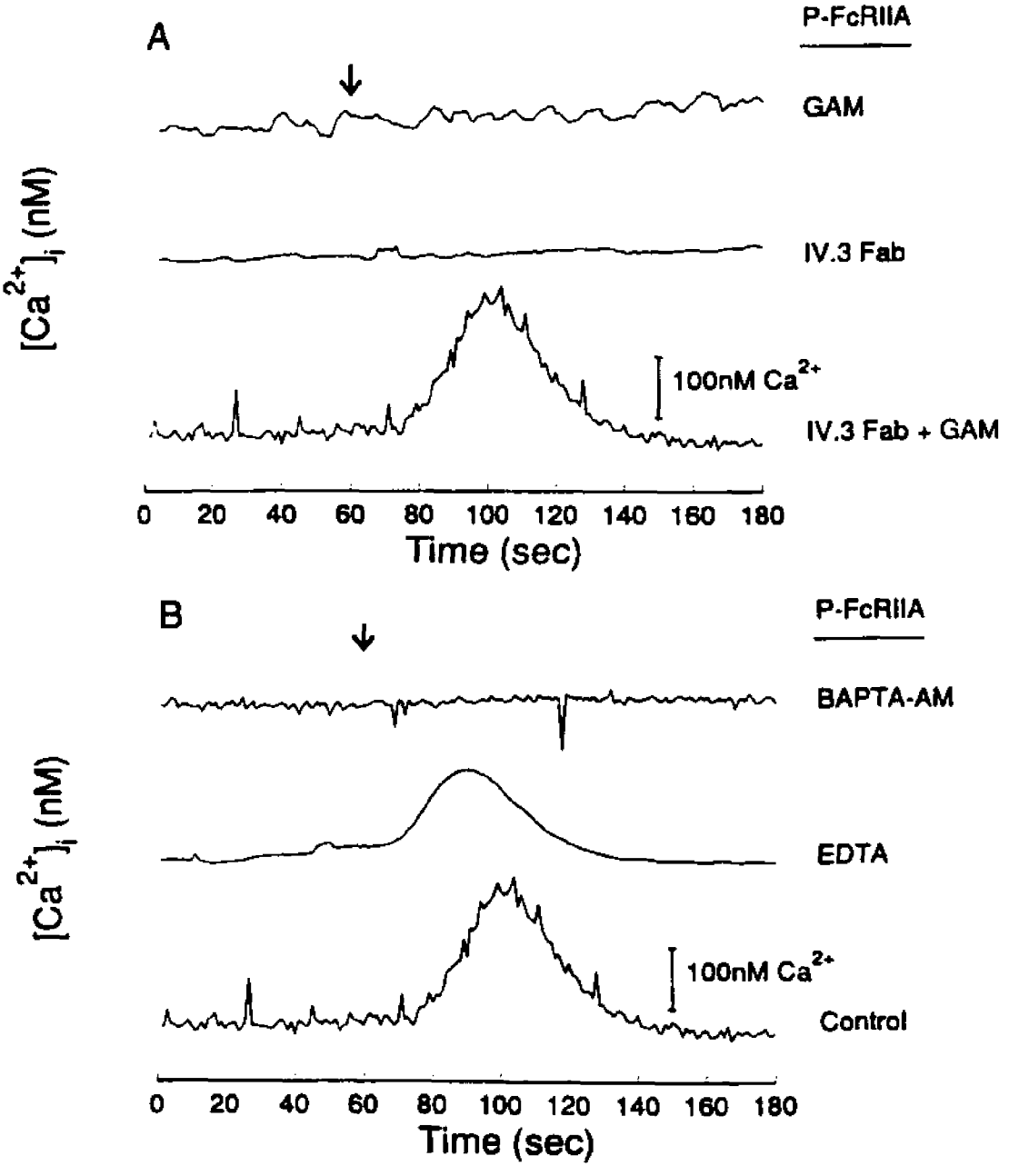


**Fig. 10.** (A) Intracellular calcium increase stimulated by cross-linking huFc$_\gamma$RIIA. Changes in intracellular calcium concentration following antibody cross-linking of huFc$_\gamma$RIIA were measured in suspensions of transfected cells that were preloaded with indo-1-AM. In control experiments only goat F(ab')$_2$ antibody to mouse IgG (GAM) or IV.3 Fab were added. (B) Effect of extracellular (EDTA) and intracellular (BAPTA-AM) free $Ca^{2+}$ chelators.

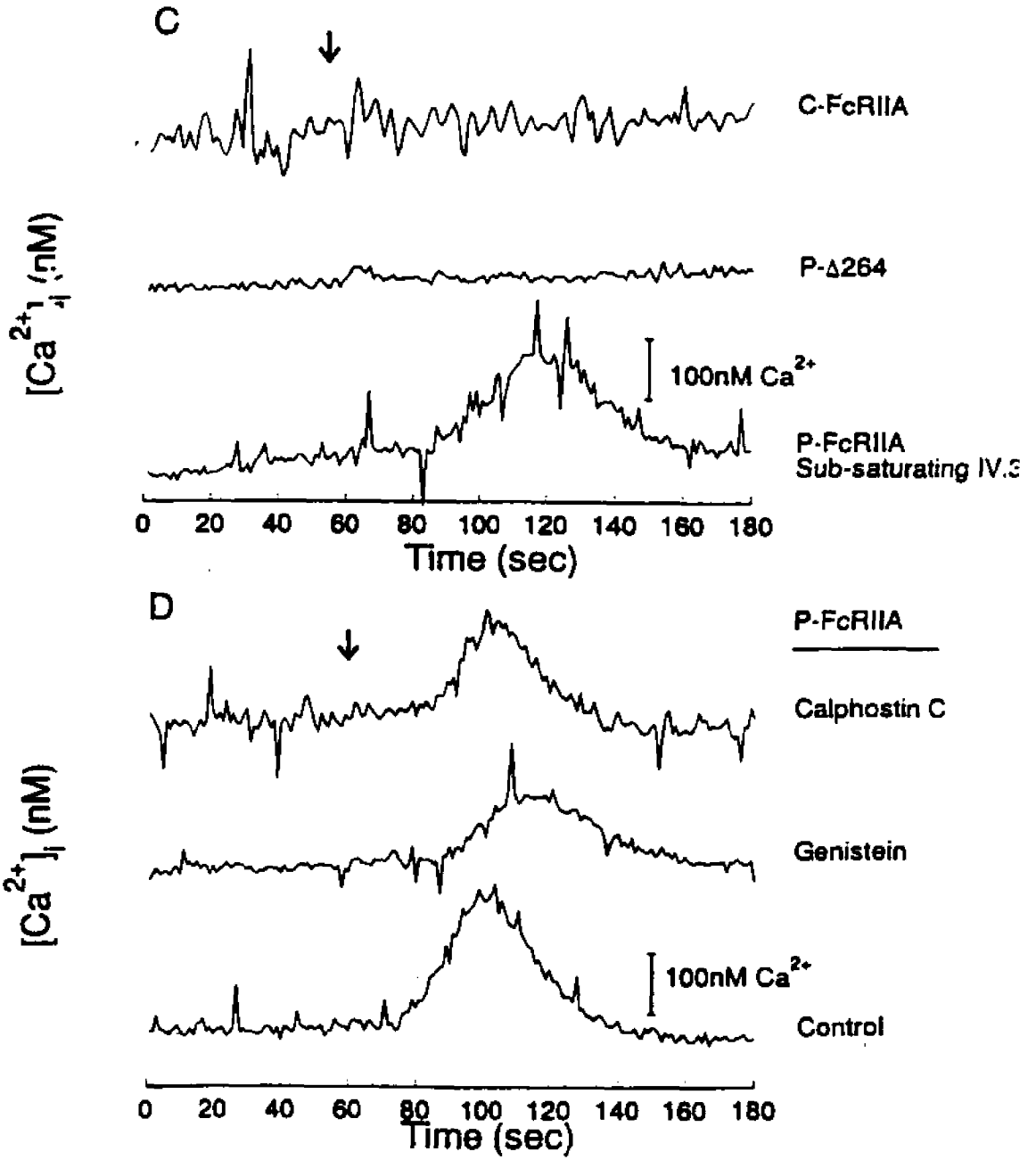


**Fig. 10.** (C) Cell type and receptor specificity. The huFc$_\gamma$RIIA-mediated $[Ca^{2+}]_i$ flux in C-FcRIIA and P-Δ264 cells is compared to that of P-FcRIIA cells labeled with a subsaturating concentration of mAb IV.3 Fab before cross-linking with GAM. (D) Effect of protein kinase C (calphostin C) and tyrosine kinase (genistein) inhibitors. All experiments were repeated at least three times on different days. Representative tracings are shown.

increase in $[Ca^{2+}]_i$. Addition of excess EDTA to chelate $Ca^{2+}$ in the buffer only partially reduced this response. In contrast, $[Ca^{2+}]_i$ did not increase in CHO cells transfected with huFc$_\gamma$RIIA, which had a baseline $[Ca^{2+}]_i$ of 157±57 nM. When the amount of mAb IV.3 Fab bound to P-FcRIIA was reduced to the amount bound to C-FcRIIA, $[Ca^{2+}]_i$ still increased after cross-linking. Thus, this huFc$_\gamma$RIIA-mediated increase in $[Ca^{2+}]_i$ comes at least partially from internal stores and requires factors found in macrophages. No cells expressing truncated huFc$_\gamma$RIIA proteins had any $[Ca^{2+}]_i$ increase. Buffering by BAPTA-AM (129) of intracellular free $Ca^{2+}$ in P-FcRIIA cells blocked any calcium increase (Fig. 10) and the internalization of labeled erythrocytes, but did not affect the rapid internalization of Ab-huFc$_\gamma$RIIA complexes (Table 2). Possibly, both the huFc$_\gamma$RIIA-mediated oxidative burst and internalization of large opsonized particles depend on an $[Ca^{2+}]_i$ flux, which was abrogated by deleting the 17 carboxyl-terminal amino acids of huFc$_\gamma$RIIA.

**Discussion**

Previous studies have analyzed internalization of cross-linked mouse Fc$_\gamma$Rs in transfected CHO cells (95,96). Cross-linked muFc$_\gamma$RII$_2$ transfected into CHO cells was internalized more efficiently than was the muFc$_\gamma$RII$_1$ splice variant, which has a 47 amino acid insertion in the cytoplasmic domain (95). These investigators suggest that muFc$_\gamma$RII$_1$, which is expressed in B cells normally (50), does not internalize efficiently since it does not localize to coated pits (95). However, both muFc$_\gamma$RII$_1$ and muFc$_\gamma$RII$_2$ expressed in CHO cells directed IgG-opsonized *Toxoplasma gondii* to lysosomes with equal efficiency (96). Since neither of these studies compared their results in CHO

cells to a similarly transfected phagocyte cell line, it is debatable whether these results reflect endocytic or phagocytic processes.

The functional comparisons between $P388D_1$ and CHO cells transfected with wild type huFc$_\gamma$RIIA indicate that the huFc$_\gamma$RIIA-mediated phagocytic response and $[Ca^{2+}]_i$ flux require macrophage signaling machinery that is not present in fibroblasts. A flux in $[Ca^{2+}]_i$ by $P388D_1$ cells expressing wild type huFc$_\gamma$RIIA, P-FcRIIA, was required for internalization of E-IV.3 Fab but not of small Ab-huFc$_\gamma$RIIA complexes. Thus, P-Δ264 cells expressing a truncated huFc$_\gamma$RIIA, which could not mediate an $[Ca^{2+}]_i$ flux, could still internalize small Ab-huFc$_\gamma$RIIA complexes, though they could not internalize E-IV.3 Fab. Greater truncation of huFc$_\gamma$RIIA abolished all phagocytic function. This differentiation between huFc$_\gamma$RII-mediated internalization of small complexes and large particles may explain some of the conflicting reports concerning the requirement of an $[Ca^{2+}]_i$ flux for huFc$_\gamma$RII-mediated phagocytosis in macrophages (101,130). Apparently, the cytoplasmic tail of huFc$_\gamma$RIIA contains distinct functional regions for initiating the internalization of small complexes versus an $[Ca^{2+}]_i$ flux and the internalization of large particles. This suggests that multiple signaling molecules interact with the cytoplasmic domain. Bifurcation of the signal pathways utilized by huFc$_\gamma$RIIA to activate multiple effectors begins at the level of the receptor.

**Materials and Methods**

*PCR amplification and subcloning of huFc$_\gamma$RIIA*

A huFc$_\gamma$RIIA cDNA clone was generously donated by J. Kochan (Hoffman La-Roche). The truncated huFc$_\gamma$RIIA cDNAs were constructed by oligonucleotide

primer-directed *in vitro* mutagenesis (114) using the polymerase chain reaction as described in Section II. All cDNAs were fully sequenced by the Brookdale Molecular Biology Center, Mount Sinai Medical Center, prior to subcloning (117) into the EcoR I site of pcEXV-3 (118) and contained only the expected mutation. pcEXV-3 is a mammalian gene expression vector with an SV-40 early gene promoter and polyadenylation signal.

*Expression of huFc$_\gamma$RIIA cDNAs*

Negative control P388D$_1$ (P-NEG) and DHFR$^-$ CHO cells (115) (C-NEG) were transfected with 1 $\mu$g/ml of a neomycin resistance gene containing vector, LKK444 (131), or a DHFR minigene, pMG1 (115), respectively, by the calcium phosphate co-precipitation method (116). Identical transfections of huFc$_\gamma$RIIA-expressing P388D$_1$ and DHFR$^-$ CHO cells were performed except for the addition of 18 $\mu$g/ml of full length or truncated huFc$_\gamma$RIIA cDNA subcloned into pcEXV-3. Transfection of P388D$_1$ cells required the addition of chloroquine (25-100 $\mu$M) to the transfection media. Transfected P388D$_1$ cells were grown in DME (Hazelton, Lenexa, KS) supplemented with 5% FCS (Intergen, Purchase, NJ) and 200 mg/L G418 (Sigma Chemical Co., St. Louis, MO). Transfected CHO cells were grown in hypoxanthine-deficient DME supplemented with 10% dialyzed FCS, 16 $\mu$M thymidine, and 300 $\mu$M proline. Suspensions of transfected cells ($2.5 \times 10^6$/ml) were incubated at 4°C with 1 $\mu$g/ml mAb IV.3 (Mederex, Inc., Hanover, NH) for 1 h, washed by centrifugation, and then labeled with 20 $\mu$g/ml FITC-conjugated goat anti-mouse IgG F(ab')$_2$ at 4°C for 1 h. After washing, 2,000 cells per sample were analyzed on a

Coulter Epics Cell Sorter. Scatchard analyses of direct binding assays utilizing $^{125}$I-mAb IV.3 ($10^6$ cpm/$\mu$g) (132) were done as previously described (120).

*Measurement of Ab-FcR complex internalization*

a) Internalization versus shedding

P-FcRIIA cells were labeled with mAb IV.3 Fab followed by either phycoerythrin (PE)-conjugated or FITC-conjugated goat anti-mouse IgG F(ab')$_2$ (Tago, Inc., Burlingame, CA) as described above. Cells were then incubated either at 4°C or 37°C for 15 min, and washed at 4°C before fluorescence analysis. Unless otherwise noted, all antibodies were purchased from Organon Teknika-Cappel, Inc. (West Chester, PA).

b) Time course

After incubation with 1 $\mu$g/ml of mAb IV.3 Fab at 4°C for 30 min, suspensions of the P-FcRIIA or C-FcRIIA cells ($2.5x10^6$/ml) were incubated with 20 $\mu$g/ml of goat anti-mouse IgG F(ab')$_2$ at 4°C for 20 min. To cross-link native muFc$_\gamma$R on P-FcRIIA cells, mAb 2.4G2 (120) and goat anti-rat IgG F(ab')$_2$ were substituted, respectively. The cells were then shifted to 37°C for the indicated time periods and washed at 4°C prior to labeling with 30 $\mu$g/ml of FITC-conjugated rabbit anti-goat IgG F(ab')$_2$ at 4°C for 30 min. To measure receptor interaction, after cross-linking either the native mouse Fc$_\gamma$R or huFc$_\gamma$RIIA and incubating the cells at 37°C, the *uncross-linked* receptor type was stained at 4°C. In all cases, background cell fluorescence was determined by omitting mAb IV.3 or mAb 2.4G2. Shifts in log fluorescence values as compared to background cell fluorescence were converted to linear fold increases in fluorescence.

The fluorescence of cells maintained at 4°C throughout was used as the control for 0% internalization. Background cell fluorescence levels represented 100% internalization. To calculate the percentage of antibody complexes internalized by labeled cells incubated at 37°C, the following equation was used: 1 - [(fold increase in fluorescence of 37°C cells - 1) ÷ (fold increase in fluorescence of 4°C cells - 1)]. Cells were maintained in 10 mM Hepes-buffered Hank's Balanced Salt Solution without $Ca^{2+}$ or $Mg^{2+}$, pH 7.5, supplemented with 0.1% dextrose and 2 mM EDTA for this procedure.

c) Internalization of truncated huFc$_\gamma$RIIA

The ability of each huFc$_\gamma$RIIA transfectant to internalize huFc$_\gamma$RII-specific or muFc$_\gamma$R-specific antibody complexes during a 15 min incubation at 37°C was calculated as described above.

d) Regulation of internalization

The ability of various transfectants to internalize antibody complexes during a 15 min incubation at 23°C versus 37°C was determined. Inhibitors were pre-incubated with the cells for 30 min at 37°C and included throughout the internalization procedure. Genistein (10 $\mu$g/ml) was purchased from UBI, Inc. (Lake Placid, NY), and Bapta-AM (100 $\mu$M) was provided by Molecular Probes, Inc. (Eugene, OR). Calphostin C (1.2 $\mu$M) was acquired from Kamiya Biomedical Co. (Thousand Oaks, CA).

*Phagocytosis of E-IV.3*

Ox erythrocytes (E) (Cornell Veterinary School) were biotinylated using sulfo-

NHS-biotin (Pierce, Co., Rockford, IL) and then incubated with streptavidin (Pierce, Co.). Opsonized E were formed by incubation of these conjugated erythrocytes with biotinylated mAb IV.3 Fab (Medarex, Inc.) or polyclonal rabbit IgG (J.C. Edberg and R.P. Kimberly, unpublished data). Opsonized E ($5.1x10^7$/ml) and huFc$_\gamma$RIIA-transfected cells ($2.2x10^6$/ml) were mixed at 4°C, pelleted, and then incubated for 20 min at 37°C to stimulate internalization. Non-internalized E were lysed by a brief incubation in hypotonic media. The percentage of cells that internalized at least one E was determined microscopically.

*Measurement of $[Ca^{2+}]i$*

Suspensions of transfected cells ($10^7$/ ml) were incubated with 5 $\mu$g/ml indo-1-AM (Molecular Probes, Inc.) for 15 min at 37°C. After the cells were washed and resuspended in a $Ca^{2+}$ and $Mg^{2+}$ free physiologic saline buffer, they were incubated with 1 $\mu$g/ml mAb IV.3 Fab (a saturating concentration) at 37°C for 5 min. The cells were next washed and resuspended in a 1.1 mM $Ca^{2+}$, 1.6 mM $Mg^{2+}$ physiologic saline buffer for 5 min at 37°C. The stirred cell suspension was then transferred to a fluorimeter to determine a resting fluorescence emission ratio (405 nm/ 490 nm) during excitation at 355 nm. After 60 s, a final concentration of 35 $\mu$g/ml of goat anti-mouse IgG F(ab')$_2$ (Tago Inc.) was added to initiate cross-linking. P-FcRIIA cells were also pre-treated with inhibitors (as described above) prior to analysis of $[Ca^{2+}]_i$. Since indo-1 fluorescence is measured at both 405 nm and 490 nm and the ratio calculated, the indo-1 signal is independent of both intracellular indo-1 concentration and cell number (127). The maximal emission ratio was determined by

lysing cells in 1% triton-X-100, and the minimal ratio by adding EDTA (40 mM). Indo-1 fluorescence emission ratios were converted to $[Ca^{2+}]_i$ using the ratio method of Grynkiewicz *et al.* (127).

## Appendix

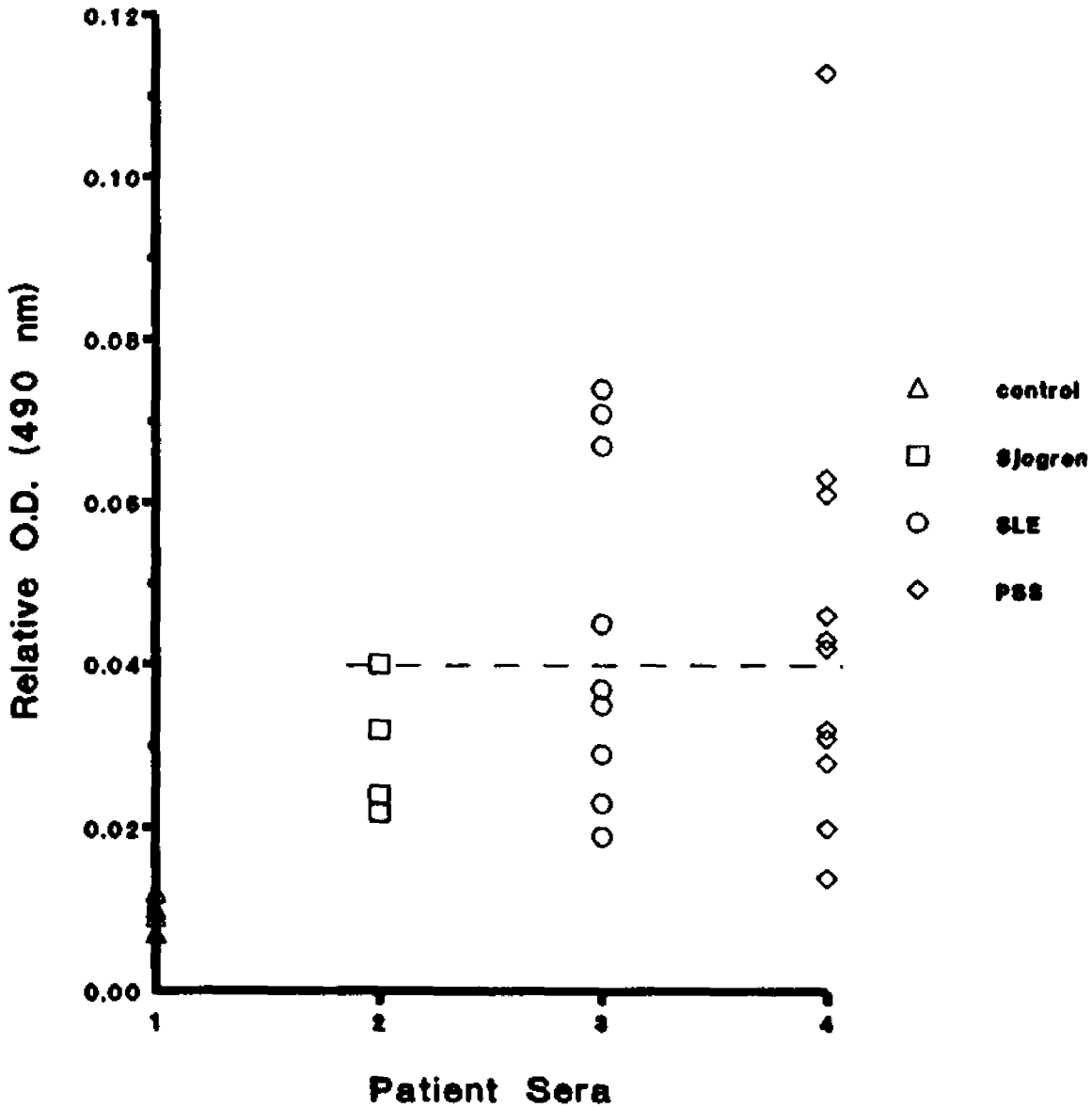


**Fig. A.** ELISA for anti-huFc$_\gamma$RIIA autoantibodies. Individual wells were coated with purified, soluble huFc$_\gamma$RIIA, and the anti-Fc$_\gamma$RIIA reactivity of sera from autoimmune patients and control individuals was determined in a colorimetric assay as described in *Materials and Methods* of Section II.

1) Primers for FcRΔ169:

TP007 TACGACTCACTATAGGGAG

MA169 TGGGCACTTAGACAGTGAT

2) Primers for FcRΔ207:

TP007 TACGACTCACTATAGGGAG

MA207 GAAATCCGCTATTTCCTGC

3) Primers for FcRΔ233:

TP007 TACGACTCACTATAGGGAG

MA233 GTTGTCTCTTTCAGATGGC

4) Primers for FcRΔ264:

TP007 TACGACTCACTATAGGGAG

MA264 GTAGATGTTTTAATCATCGTC

**Fig. B.** Oligonucleotide primer sequences used to construct truncated huFc$_\gamma$RIIA cDNAs. The TP007 primer (the sense primer in all cases) corresponds to the PGEM-4 sequence which was immediately 5′ of the huFc$_\gamma$RIIA insert. The mutant antisense (MA#) primers are numbered for the huFc$_\gamma$RIIA codon (see Fig. 1) at which the new protein will terminate. The mutant nucleotide base in each antisense primer is shown in bold type.

## Bibliography

1. P. Boros, J. Chen, C. Bona, J. C. Unkeless, *J. Exp. Med.* **171**, 1581 (1990).

2. J. A. Odin, C. J. Painter, J. C. Unkeless, in *Cellular and Molecular Mechanisms of Inflammation. Receptors on Inflammatory Cells: Structure-Function Relationships*, C. G. Cochrane and Jr. Gimbrone, M.A., Eds. (Academic Press, Inc., San Diego, 1990), p. 1.

3. J. L. Teillaud, C. Mathiot, S. Ameigorena, S. Brunati, J. Moncuit, et al, in *Cancer Detection and Prevention*, (Liss, New York, 1987).

4. N. E. Phillips, D. C. Parker, *J. Immunol.* **134**, 2835 (1985).

5. N. E. Simister, K. E. Mostov, *Nature* **337**, 184 (1989).

6. S. G. Stuart, N. E. Simister, S. B. Clarkson, B. M. Kacinski, M. Shapiro, et al, *EMBO J.* **8**, 3657 (1989).

7. R. Hoffman, R. A. Briddell, K. Van Besien, E. F. Srour, T. Guscar, et al, *N. Engl. J. Med.* **321**, 97 (1989).

8. S. B. Clarkson, R. P. Kimberly, J. E. Valinsky, M. D. Witmer, J. B. Bussel, et al, *J. Exp. Med.* **164**, 474 (1986).

9. A. Sipos, C. Csortos, S. Sipka, P. Gergely, I. Sonkoly, et al, *Immunol. Lett.* **19**, 329 (1988).

10. P. Selvaraj, W. F. Rosse, R. Silber, T. A. Springer, *Nature* **333**, 565 (1988).

11. T. W. Huizinga, C. E. van der Schoot, C. Jost, R. Klaassen, M. Kleijer, et al, *Nature* **333**, 667 (1988).

12. J. V. Ravetch, B. Perussia, *J. Exp. Med.* **170**, 481 (1989).

13. B. J. Scallon, E. Scigliano, V. H. Freedman, M. C. Miedel, Y. -C. E. Pan, et al, *Proc. Natl. Acad. Sci. USA* **86**, 5079 (1989).

14. E. Ueda, T. Kinoshita, J. Nojima, K. Inoue, T. Kitani, *J. Immunol.* **143**, 1274 (1989).

15. R. J. Kurlander, J. Batker, *J. Clin. Invest.* **69**, 1 (1982).

16. L. F. Fries, R. P. Hall, T. J. Lawley, G. R. Crabtree, M. M. Frank, *J. Immunol.* **129**, 1041 (1982).

17. M. D. Lubeck, Z. Steplewski, F. Baglia, M. H. Klein, K. J. Dorrington, et al, *J. Immunol.* **135**, 1299 (1985).

18. J. H. O'Grady, R. J. Looney, C. L. Anderson, *J. Immunol.* **137**, 2307 (1986).

19. C. L. Anderson, *J. Exp. Med.* **156**, 1794 (1982).

20. L. Cohen, S. Sharp, A. Kulczycki, Jr., *J. Immunol.* **131**, 378 (1983).

21. J. Frey, W. Engelhardt, *Eur. J. Immunol.* **17**, 583 (1987).

22. G. Peltz, K. Frederick, C. L. Anderson, B. M. Peterlin, *Mol. Immunol.* **25**, 243 (1988).

23. K. C. Petroni, L. Shen, P. M. Guyre, *J. Immunol.* **140**, 3467 (1988).

24. B. Perussia, E. T. Dayton, R. Lazarus, V. Fanning, G. Trinchieri, *J. Exp. Med.* **158**, 1092 (1983).

25. J. M. Allen, B. Seed, *Science* **243**, 378 (1989).

26. D. W. Sears, N. Osman, B. Tate, I. F. C. McKenzie, P. M. Hogarth, *J. Immunol.* **144**, 371 (1990).

27. D. H. Jones, R. J. Looney, C. L. Anderson, *J. Immunol.* **135**, 3348 (1985).

28. A. Kulczycki, Jr., *J. Immunol.* **133**, 849 (1984).

29. R. J. Looney, D. H. Ryan, K. Takahashi, H. B. Fleit, H. J. Cohen, et al, *J. Exp. Med.* **163**, 826 (1986).

30. L. M. Anselmino, B. Perussia, L. L. Thomas, *J. Allergy Clin. Immunol.* **84**, 907 (1989).

31. S. P. Karas, W. F. Rosse, R. J. Kurlander, *Blood* **60**, 1277 (1982).

32. M. L. Hibbs, L. Bonadonna, B. M. Scott, I. F. McKenzie, P. M. Hogarth, *Proc. Natl. Acad. Sci. USA* **85**, 2240 (1988).

33. S. G. Stuart, M. L. Trounstine, D. J. Vaux, T. Koch, C. L. Martens, et al, *J. Exp. Med.* **166**, 1668 (1987).

34. R. J. Looney, G. N. Abraham, C. L. Anderson, *J. Immunol.* **136**, 1641 (1986).

35. T. Seki, *Immunogenetics.* **30**, 5 (1989).

36. D. G. Brooks, W. Q. Qiu, A. D. Luster, J. V. Ravetch, *J. Exp. Med.* **170**, 1369 (1989).

37. S. Stengelin, I. Stamenkovic, B. Seed, *EMBO. J.* **7**, 1053 (1988).

38. C. L. Anderson, *Clin. Immunol. Immunopathol.* **53**, S63 (1989).

39. H. B. Fleit, S. D. Wright, J. C. Unkeless, *Proc. Natl. Acad. Sci. USA* **79**, 3275 (1982).

40. L. L. Lanier, J. J. Ruitenberg, J. H. Phillips, *J. Immunol.* **141**, 3478 (1988).

41. J. C. Edberg, P. B. Redecha, J. E. Salmon, R. P. Kimberly, *J. Immunol.* **143**, 1642 (1989).

42. P. Selvaraj, O. Carpen, M. L. Hibbs, T. A. Springer, *J. Immunol.* **143**, 3283 (1989).

43. T. Kurosaki, J. V. Ravetch, *Nature* **342**, 805 (1989).

44. L. L. Lanier, S. Cwirla, G. Yu, R. Testi, J. H. Phillips, *Science* **246**, 1611 (1989).

45. P. Lalezari, M. Khorshidi, M. Petrosova, *J. Pediatr.* **109**, 764 (1986).

46. J. C. Unkeless, *Curr. Opinion Immunol.* **2**, 63 (1989).

47. J. C. Unkeless, H. N. Eisen, *J. Exp. Med.* **142**, 1520 (1975).

48. J. C. Unkeless, *J. Exp. Med.* **145**, 931 (1977).

49. I. S. Mellman, J. C. Unkeless, *J. Exp. Med.* **152**, 1048 (1980).

50. J. V. Ravetch, A. D. Luster, R. Weinshank, J. Kochan, A. Pavlovec, et al, *Science* **234**, 718 (1986).

51. Z. Qu, J. Odin, J. D. Glass, J. C. Unkeless, *J. Exp. Med.* **167**, 1195 (1988).

52. M. L. Hibbs, B. J. Classon, I. D. Walker, I. F. McKenzie, P. M. Hogarth, *J. Immunol.* **140**, 544 (1988).

53. R. L. Weinshank, A. D. Luster, J. V. Ravetch, *J. Exp. Med.* **167**, 1909 (1988).

54. C. Bonnerot, M. Daeron, N. Varin, S. Amigorena, P. M. Hogarth, et al, *J. Immunol.* **141**, 1026 (1988).

55. C. Bonnerot, S. Amigorena, W. H. Fridman, J. Even, M. Daëron, *J. Immunol.* **144**, 323 (1990).

56. B. Perussia, M. M. Tutt, W. Q. Qiu, W. A. Kuziel, P. W. Tucker, et al, *J. Exp. Med.* **170**, 73 (1989).

57. A. Santiago, J. Satriano, S. DeCandido, H. Holthofer, R. Schreiber, et al, *J. Immunol.* **143**, 2575 (1989).

58. U. Blank, C. Ra, L. Miller, K. White, H. Metzger, et al, *Nature* **337**, 187 (1989).
59. C. Ra, M. H. E. Jouvin, U. Blank, J. P. Kinet, *Nature* **341**, 752 (1989).

60. M. L. Hibbs, P. Selvaraj, O. Carpen, T. A. Springer, H. Kuster, et al, *Science* **246**, 1608 (1989).

61. L. L. Lanier, G. Yu, J. H. Phillips, *Nature* **342**, 803 (1989).

62. P. Anderson, M. Caligiuri, C. O'Brien, T. Manley, J. Ritz, et al, *Proc. Natl. Acad. Sci. USA* **87**, 2274 (1990).

63. T. Kurosaki, I. Gander, J. V. Ravetch, *Proc. Natl. Acad. Sci. USA* **88**, 3837 (1991).

64. S. J. Frank, B. B. Niklinska, D. G. Orloff, M. Mercep, J. D. Ashwell, et al, *Science* **249**, 174 (1990).

65. C. L. Anderson, P. M. Guyre, J. C. Whitin, D. H. Ryan, R. J. Looney, et al, *J. Biol. Chem.* **261**, 12856 (1986).

66. L. C. Pfefferkorn, M. W. Fanger, *J. Biol. Chem.* **264**, 14112 (1989).

67. M. F. Tosi, M. F. Berger, *J. Immunol.* **141**, 2097 (1988).

68. T. W. J. Huizinga, F. van Kemenade, L. Koenderman, K. M. Dolman, A. E. von dem Borne, et al, *J. Immunol.* **142**, 2365 (1989).

69. L. Shen, R. F. Graziano, M. W. Fanger, *Mol. Immunol.* **26**, 959 (1989).

70. M. W. Fanger, L. Shen, R. F. Graziano, P. M. Guyre, *Immunol. Today* **10**, 92 (1989).

71. R. F. Graziano, D. V. Erbe, M. W. Fanger, *J. Immunol.* **143**, 3894 (1989).

72. R. W. Leu, A. Zhou, J. A. Rummage, M. J. Kennedy, B. J. Shannon, *J. Immunol.* **143**, 3250 (1989).

73. Y. Akiyama, M. D. Lubeck, Z. Steplewski, H. Koprowski, *Cancer Research* **44**, 5127 (1984).

74. L. Shen, P. M. Guyre, M. W. Fanger, *J. Immunol.* **139**, 534 (1987).

75. R. F. Graziano, M. W. Fanger, *J. Immunol.* **139**, 3536 (1987).

76. J. H. A. Boot, M. E. J. Geerts, L. A. Aarden, *J. Immunol.* **142**, 1217 (1989).

77. R. F. Graziano, R. J. Looney, L. Shen, M. W. Fanger, *J. Immunol.* **142**, 230 (1989).

78. T. Werfel, P. Uciechowski, P. A. T. Tetteroo, R. Kurrle, H. Diecher, et al, *J. Immunol.* **142**, 1102 (1989).

79. I. Anegon, M. C. Cuturi, G. Trinchieri, B. Perussia, *J. Exp. Med.* **167**, 452 (1988).

80. R. J. L. Klaassen, W. H. Ouwehand, T. W. J. Huizinga, C. P. Engelfriet, A. E. G. K. Von dem Borne, *J. Immunol.* **144**, 599 (1990).

81. J. C. Cerrottini, K. T. Brunner, *Adv. Immunol.* **18**, 67 (1974).

82. C. Nathan, Z. Cohn, *J. Exp. Med.* **152**, 198 (1980).

83. C. Nathan, L. Brukner, G. Kaplan, J. Unkeless, Z. Cohn, *J. Exp. Med.* **152**, 183 (1980).

84. W. A. Kuziel, A. Takashima, M. Bonyhadi, P. R. Bergstresser, J. P. Allison, et al, *Nature* **328**, 263 (1987).

85. C. L. Anderson, L. Shen, *FASEB. J.* **3**, A1104 (1985), abstract.

86. R. A. Ezekowitz, J. Austyn, P. D. Stahl, S. Gordon, *J. Exp. Med.* **154**, 60 (1981).

87. J. Schneck, O. M. Rosen, B. Diamond, B. R. Bloom, *J. Immunol.* **126**, 745 (1981).

88. A. Yamada, K. N. Dileepan, D. J. Stechschulte, T. Suzuki, *J. Mol. Cell Immunol.* **4**, 191 (1989).

89. R. J. Kurlander, J. Hall, *J. Clin. Invest.* **77**, 2010 (1986).

90. R. J. Kurlander, D. M. Ellison, J. Hall, *J. Immunol.* **133**, 855 (1984).

91. S. B. Clarkson, J. B. Bussel, R. P. Kimberly, J. E. Valinsky, R. L. Nachman, et al, *N. Engl. J. Med.* **314**, 1236 (1986).

92. N. E. Phillips, K. A. Gravel, K. Tumas, D. C. Parker, *J. Immunol.* **141**, 4243 (1989).

93. G. Laszlo, H. B. Dickler, *J. Immunol.* **141**, 3416 (1988).

94. W. Hunziker, I. Mellman, *J. Cell Biol.* **109**, 3291 (1989).

95. H. M. Miettinen, J. K. Rose, I. Mellman, *Cell* **58**, 317 (1989).

96. K. A. Joiner, S. A. Fuhrman, H. M. Miettinen, L. H. Kasper, I. Mellman, *Science* **249**, 641 (1990).

97. H. Metzger, J. P. Kinet, *FASEB. J.* **2**, 3 (1988).

98. D. V. Erbe, E. R. Pfefferkorn, M. W. Fanger, *J. Immunol.* **146**, 3145 (1991).

99. A. A. Aderem, W. A. Scott, Z. A. Cohn, *J. Exp. Med.* **163**, 139 (1986).

100. D. P. Lew, *Eur. J. Clin. Invest.* **19**, 338 (1989).

101. F. Di Virgilio, B. C. Meyer, S. Greenberg, S. C. Silverstein, *J. Cell Biol.* **106**, 657 (1988).

102. G. Trinchieri, T. O'Brien, M. Shade, B. Perussia, *J. Immunol.* **133**, 1869 (1984).

103. E. A. MacIntyre, P. J. Roberts, R. Abdul-Gaffar, K. O'Flynn, G. R. Pilkington, et al, *J. Immunol.* **141**, 4333 (1988).

104. H. E. Willis, B. Browder, A. J. Feister, T. Mohanakumar, S. Ruddy, *J. Immunol.* **140**, 234 (1988).

105. W. D. Blackburn, Jr., L. W. Heck, *Biochem. Biophys. Res. Commun.* **164**, 983 (1989).

106. R. I. Sha'afi, J. R. White, T. F. P. Molski, J. Shefcyk, M. Volpi, et al, *Biochem. Biophys. Res. Commun.* **114**, 638 (1983).

107. R. R. Almon, C. G. Andrew, S. H. Appel, *Science* **186**, 55 (1974).

108. M. J. Caulfield, D. Stanko, C. Calkins, *Immunology.* **66**, 233 (1989).

109. M. M. Frank, T. J. Lawley, M. I. Hamburger, E. J. Brown, *Ann. Intern. Med.* **98**, 206 (1983).

110. P. J. Russell, A. D. Steinberg, *Clin. Immunol. Immunopathol.* **27**, 387 (1983).

111. B. Perussia, G. Trinchieri, *J. Immunol.* **132**, 1410 (1984).

112. P. J. Russell, F. H. Cameron, *J. Leukoc. Biol.* **39**, 49 (1986).

113. P. Boros, J. A. Odin, T. Muryoi, S. K. Masur, C. Bona, et al, *J. Exp. Med.* **173**, 1473 (1991).

114. A. Hemsley, N. Arnheim, M. D. Toney, G. Cortopassi, D. J. Galas, *Nucleic. Acids. Res.* **17**, 6545 (1989).

115. G. Urlaub, P. J. Mitchell, E. Kas, L. A. Chasin, V. L. Funanage, et al, *Somatic Cell. Mol. Genet.* **12**, 216 (1986).

116. M. Wigler, A. Pellicer, S. Silverstein, R. Axel, G. Urlaub, et al, *Proc. Natl. Acad. Sci. USA* **76**, 1373 (1979).

117. T. Maniatis, E. F. Frisch, J. Sambrook, *Molecular Cloning: A Laboratory Manual* (Cold Spring Harbor, New York, 1982).

118. J. Miller, T. R. Malek, W. J. Leonard, W. C. Greene, E. M. Shevach, et al, *J. Immunol.* **134**, 4212 (1985).

119. D. M. Neville, *J. Biol. Chem.* **246**, 6328 (1971).

120. J. C. Unkeless, *J. Exp. Med.* **150**, 580 (1979).

121. M. M. Martin, L. Lindqvist, *J. Luminesc.* **10**, 381 (1975).

122. P. Midoux, A. -C. Roche, M. Monsigny, *Cytometry.* **8**, 327 (1987).

123. E. Holtzman, in *Lysosomes*, (Plenum Press, New York, 1989), ch. 4.

124. T. Andersson, M. Fallman, D. P. Lew, O. Stendahl, *FEBS Lett.* **239**, 371 (1988).

125. H. D. Gresham, A. Zheleznyak, J. S. Mormol, E. J. Brown, *J. Biol. Chem.* **265**, 7819 (1990).

126. P. A. Connelly, C. A. Farrell, J. M. Merenda, M. J. Conklyn, H. J. Showell, *Biochem. Biophys. Res. Commun.* **177**, 192 (1991).

127. G. Grynkiewicz, M. Poenie, R. Y. Tsien, *J. Biol. Chem.* **260**, 3440 (1985).

128. R. P. Kimberly, J. W. Ahlstrom, M. E. Click, J. C. Edberg, *J. Exp. Med.* **171**, 1239 (1990).

129. H. M. Korchak, L. B. Vosshall, K. A. Haines, C. Wilkenfeld, K. F. Lundquist, et al, *J. Biol. Chem.* **263**, 11098 (1988).

130. D. H. Munn, M. McBride, N. -K. V. Cheung, *Cancer Res.* **51**, 1117 (1991).

131. P. Gunning, J. Leavitt, G. Muscat, S. Ng, L. Kedes, *Proc. Natl. Acad. Sci. USA* **84**, 4831 (1987).

132. P. J. Fraker, J. C. Speck, Jr., *Biochem. Biophys. Res. Commun.* **80**, 849 (1978).